A NEW MODEL FOR THE QUEBECIA TERRANE IN THE GRENVILLE PROVINCE AS A COMPOSITE ARC BELT: SM-ND EVIDENCE

A NEW MODEL FOR THE QUEBECIA TERRANE IN THE GRENVILLE PROVINCE AS A COMPOSITE ARC BELT: SM-ND EVIDENCE

BY

SHANNON VAUTOUR, B.Sc. (Hons.)

A Thesis

Submitted to the School of Graduate Studies

In Partial Fulfillment of the Requirements

For the Degree

Master of Science

McMaster University

MASTER OF SCIENCE (2015) MCMASTER UNIVERSITY

(Geology) Hamilton, Ontario

TITLE:	A New model for the Quebecia Terrane in the Grenville Province as a composite arc belt: Sm-Nd evidence
AUTHOR:	Shannon Vautour, B.Sc. (McMaster University)
SUPERVISOR:	Professor Alan P. Dickin
NUMBER OF PAGES:	66

Abstract

The Grenville Province represents a complex, highly metamorphosed orogenic belt at the southeastern margin of the Canadian Shield that is composed of different lithotectonic domains of various ages that have all been affected by the 1.0 Ga Grenville Orogeny. The present study focuses on one of the youngest regions, the Quebecia terrane, and through reconnaissance neodymium isotope mapping, investigates the extent of an old crustal block that predates the Grenville Orogeny.

The Quebecia Terrane is found within Central Quebec and is a Mesoproterozoic arc terrane that was constructed around 1.5 Ga. Utilizing the Samarium-Neodymium dating method, previous research had identified a few isolated neodymium signatures of older crustal ages, and through reconnaissance mapping, several of these Paleoproterozoic crustal blocks are suggested to represent a single fragmented crustal panel. The study focused on more detailed mapping of these blocks in the areas of Baie Comeau, Forestville, Labrieville and Pipmuacan in Central Quebec.

The full extent and connection between the fragments has been mapped as a series of Paleoproterozoic crustal blocks extending longitudinally through the Quebecia terrane. These blocks are embedded within the younger terrane, suggesting that the old panel was incorporated sometime during the accretion of Quebecia to Laurentia. It is possible that the old panel broke off from older Laurentian crust and reattached during the accretion of the Quebecia terrane via strike slip tectonics, implying that the Quebecia terrane itself consists of more than one accreted unit. The present study found that the older neodymium isotope signatures were consistent with the Berthe Terrane in the

Manicouagan region to the north, providing evidence for the origin of the older panel within Quebecia. However, by invoking a division of Quebecia into a north and south segment, this implies a Composite Arc Belt model for the Central Grenville Province.

Acknowledgements

I would first like to express my sincere gratitude to my supervisor, Dr. Alan P Dickin, for taking me on as his B.Sc undergraduate and M.Sc student, and for showing me the beautiful province of Quebec through our many exciting field work excursions. Thanks to his guidance, support and unwavering patience with me (and many, many coffee breaks), I successfully made it to where I am today in academia.

I would also like to thank my lab family who helped me learn and grow these past four years: First to my predecessor, Dr. Rebecca Moumblow, who served as both my role model and good friend, for influencing me to go farther in my degree, and teaching me the ropes of graduate student life. Second, to Gabriel Arcuri, for the Starbucks dates and vent sessions, and for keeping me calm and level headed when writing got stressful. Lastly, to Jacob Strong, for being a GIS master and helping me with my interpolations, and always providing a good laugh in the lab. Thank you all so much for your support, smiles and guidance.

A special thank you to my parents, Kelly and Garth Vautour, who although may not have understood many of the geologic terms as I anxiously practiced my presentations in front of them, consistently gave me amazing support, understanding and love throughout this whole journey. I could not have done it without you all!

Table of Contents

List of Tables

List of Figures

Chapter 1: Geological History

1.1 Introduction

The Canadian Shield is the oldest portion of the North American crustal plate. It is largely comprised of exposed Precambrian rock and covers much of the eastern half of Canada and part of the northern United States. The shield is divided into several provinces of various geologic ages, where the Grenville Province is not only the youngest, but also the most complex. The Grenville Province records about one billion years of crustal growth, from 2 Ga – 1 Ga, culminating with the formation of the supercontinent Rodinia.

The concept of supercontinents was first developed by Alfred Wegener, based on his theory of continental drift (Wegener, 1929). He proposed that prior to their present day distribution, Earth's continents were once assembled into one large supercontinent 300 million years ago, which he named Pangaea. Canadian geologist J. Tuzo Wilson was one of the first scientists to suggest that there may have been ancient oceans that were destroyed by the formation of Pangaea, leading to suspicions that this could only be true if there were also ancient supercontinents prior to Pangaea (Wilson, 1966).

The configuration of Pangaea is well established based on patterns of fossil evidence, oceanic magnetic anomalies, and the fit of modern continents to each other. However, because of the older age of the ancient pre-Pangaea supercontinents, the evidence is less certain, making it more difficult to propose configurations.

1.2 Precambrian Supercontinents

Evidence began to surface in the early 1970's for a ~1 Ga supercontinent, variously called "proto-Pangaea" (Sawkins, 1976) or simply, "the Late Proterozoic Supercontinent" (Piper, 1987). While studying the Cambrian explosion and the environmental conditions prior to Pangaea, McMenamin and McMenamin (1990) noted that paleomagnetic evidence, Precambrian bedrock geology and paleobiogeography supported the existence of a pre-Pangaea supercontinent and they named it Rodinia. The first proposed assembly for Rodinia is shown in Figure 1.1.

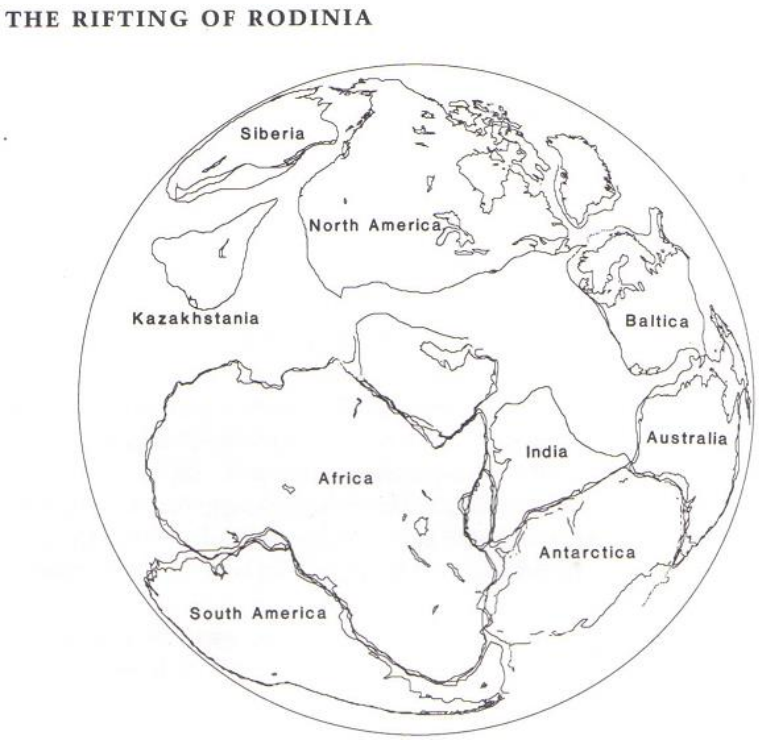

Figure 1.1: The first proposed Rodinia assembly, surrounded by the superocean Mirovia (McMenamin and McMenamin, 1990)

After the acceptance of this new supercontinent, studies showed that similar processes had occurred to create and destroy the two ancient supercontinents Pangaea and Rodinia. It was therefore suggested that the timeline of supercontinent growth followed three

stages: (1) an initial period of accretion, (2) an intermediate period of accretion in some areas until the achievement of maximum ‘packing’, while rifting began in others, and (3) a final period of complete fragmentation due to rifting (Rogers and Santosh, 2002).

After a decade of studies providing more solid evidence for Rodinia’s existence, it began to seem likely that Rodinia formed from accretion of fragments from an even older Paleoproterozoic supercontinent, with the addition of several juvenile crustal blocks. In 2002, Rogers and Santosh proposed an older supercontinent called Columbia.

In the Paleoproterozoic, it is proposed that Columbia, more commonly referred to today as Nuna, was formed from a linear arrangement of older cratons, Laurentia, Baltica and Amazonia (Figure 1.2).

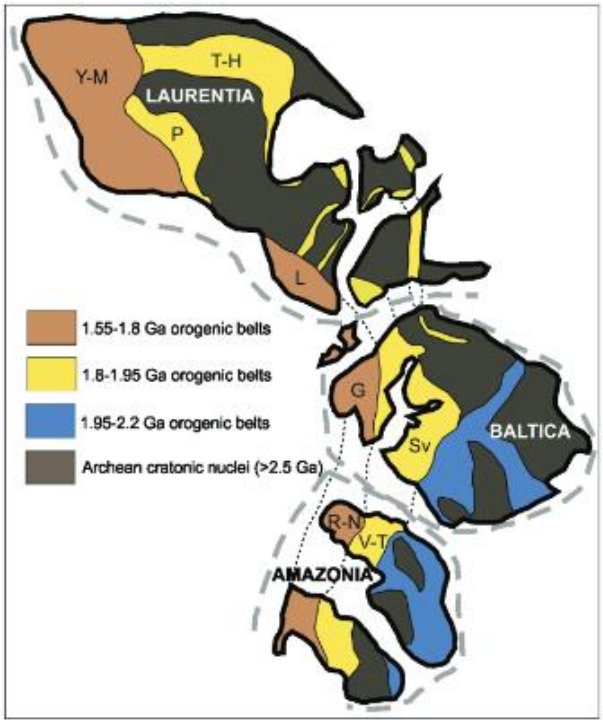

Figure 1.2: Possible craton assembly of Nuna around 1.54 Ga; Y-M: Yavapai-Mazatzal, T-H: Trans-Hudson, P: Penokean, L: Labradorian, G: Grenvillian, Sv: Svecofennian, R-N: Rio Negro-Juruena, V-T: Ventuari-Tapajos (Pesonen et al., 2012).

During the Mesoproterozoic around 1.6 Ga, Nuna had reached its maximum size (Rogers and Santosh, 2002), after which its component parts, Laurentia, Baltica and Amazonia, with the addition of the West African craton, would later be the basis for the Neoproterozoic supercontinent, Rodinia (Figure 1.3, Pesonen et al., 2012).

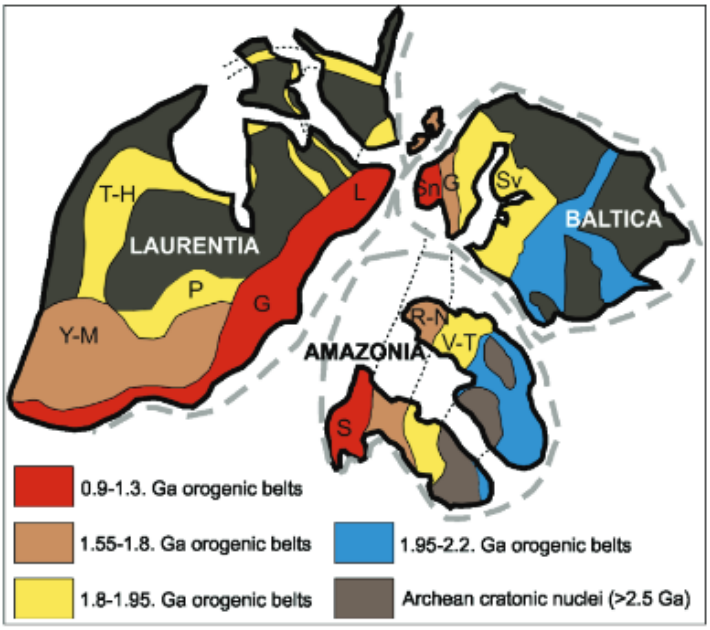

Figure 1.3: Possible craton assembly of Rodinia around 1.04 Ga; Y-M: Yavapai-Mazatzal, T-H: Trans-Hudson, P: Penokean, L: Labradorian, G: Grenvillian, Sv: Svecofennian, Sn: Sveconorwegian, S: Sunsas, R-N: Rio Negro-Juruena, V-T: Ventuari-Tapajos (Pesonen et al., 2012).

After the amalgamation of the supercontinent Nuna, and before the formation of the supercontinent Rodinia, there were five long-lived > 500 Myr accretionary orogenic events between the two supercontinent assemblies. However, Condie (2013) grouped four of these, Penokean-Yavapai-Mazatzal, Makkovikian-Labradorian, Baltica, and Amazonia, into the Great Proterozoic Accretionary Orogen (GPAO). This is said to possibly be the

long-lived orogen of all time, and contributed to much of the Rodinia supercontinent (Condie, 2013).

Condie (2013) summarized zircon ages from igneous rocks preserved in the Laurentian portion of the GPAO – Figure 1.4 is a distribution map of the zircon ages within the Laurentian portion of the GPAO, and Figure 1.5 is the histogram of the age data.

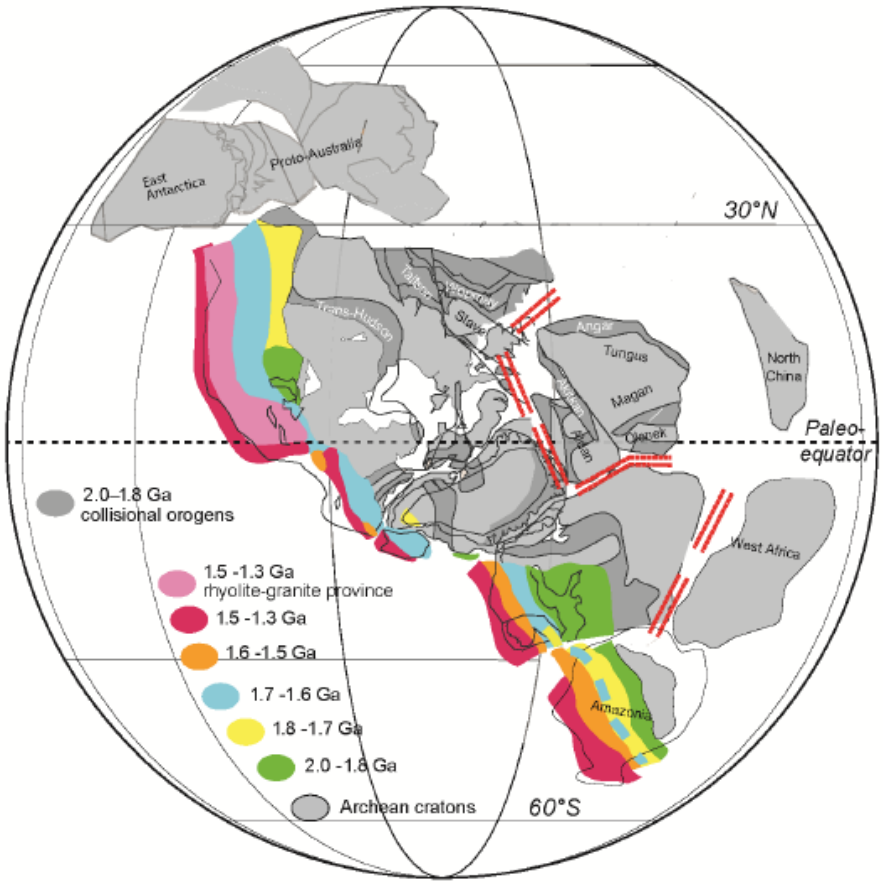

Figure 1.4: Paleomagnetic reconstruction of Nuna at the beginning of its break-up phase showing age provinces in the GPAO using detrital zircon ages. Double red lines: rifting of cratons (Condie, 2013).

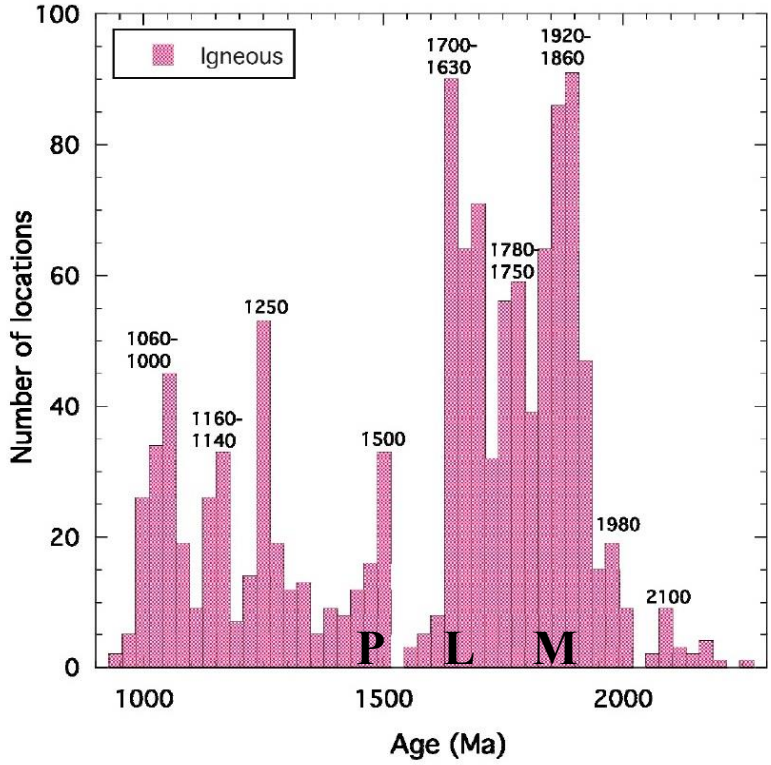

Figure 1.5: Worldwide zircon ages from igneous rocks preserved in the Laurentian portion of the GPAO in MA (Condie, 2013) P=Pinwarian age, L=Labradorian age, M=Makkovikian age

Several of the maxima he identified correlate directly with North American orogenic events, such as the 1.5 Ga Pinwarian, 1.7-1.63 Ga Labradorian, and 1.92-1.86 Ga Makkovikian (Figure 1.5). However, an unexplained minimum at 1.6-1.5 Ga was observed between Labradorian and Pinware orogenic events. Condie (2013) suggested this gap in Uranium-Lead (U-Pb) dating between Labradorian and Pinware orogenic events could be explained by three scenarios: (1) rocks of this age never formed, (2) rocks of this age are covered with younger rocks, (3) rocks of this age were recycled into the mantle; where the latter is Condie's preferred explanation for the gap. The Grenville Province provides the largest exposure of Mesoproterozoic basement in North America,

therefore further study of Mesoproterozoic crustal formation in the Grenville Province may offer a chance to solve this problem.

1.3 The Grenville Province

The Grenville Province forms a longitudinal belt 2000 km long and 400 km wide, extending through Ontario and Quebec, from Georgian Bay to Labrador. The province represents a complex, highly metamorphosed orogenic belt at the southeastern margin of the Canadian Shield. The Grenville province is bounded to the north by the Grenville Front, which is juxtaposed against the Archean aged Superior Province (Figure 1.6).

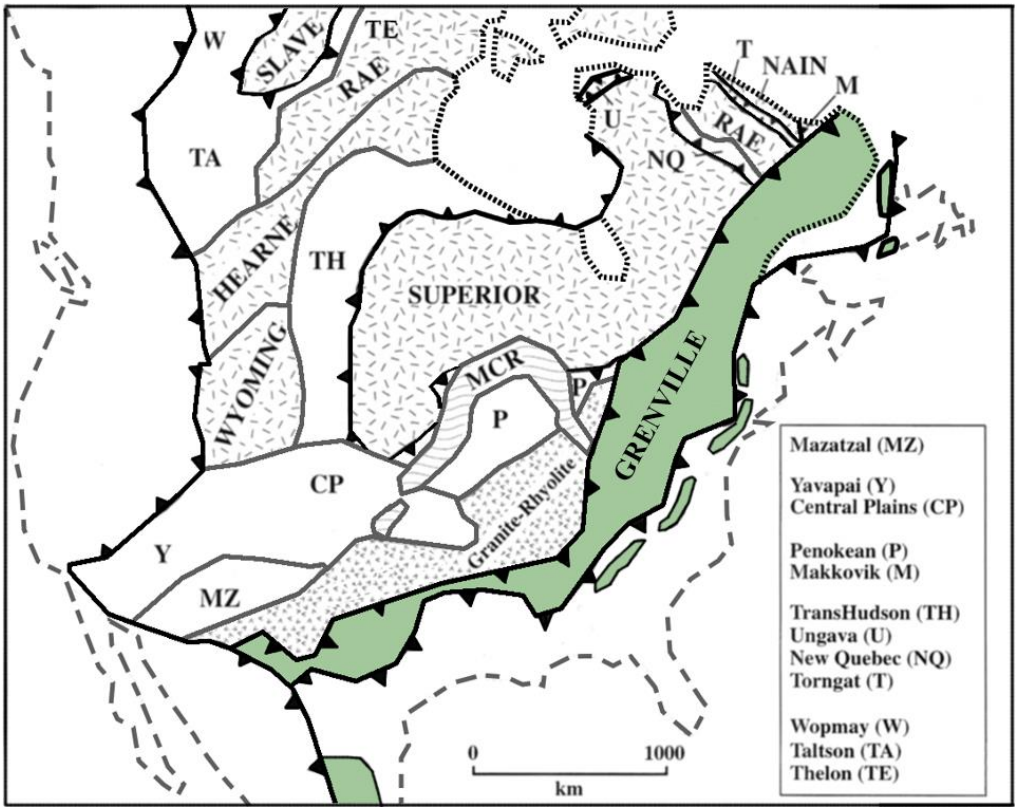

Figure 1.6: Geologic divisions of the North American Shield with the Grenville Province highlighted in green; dashed lines indicating coastlines (after Rivers, 1997)

There have been several different divisions of the Grenville Province; Wynne-Edwards (1972) had presented seven broad divisions based on metamorphic grades when little else was known about the province, but this was superseded by the model of Rivers et al. (1989), who divided the province into three tectonic structural belts based on geologic, geophysical and geochronological evidence (Figure 1.7).

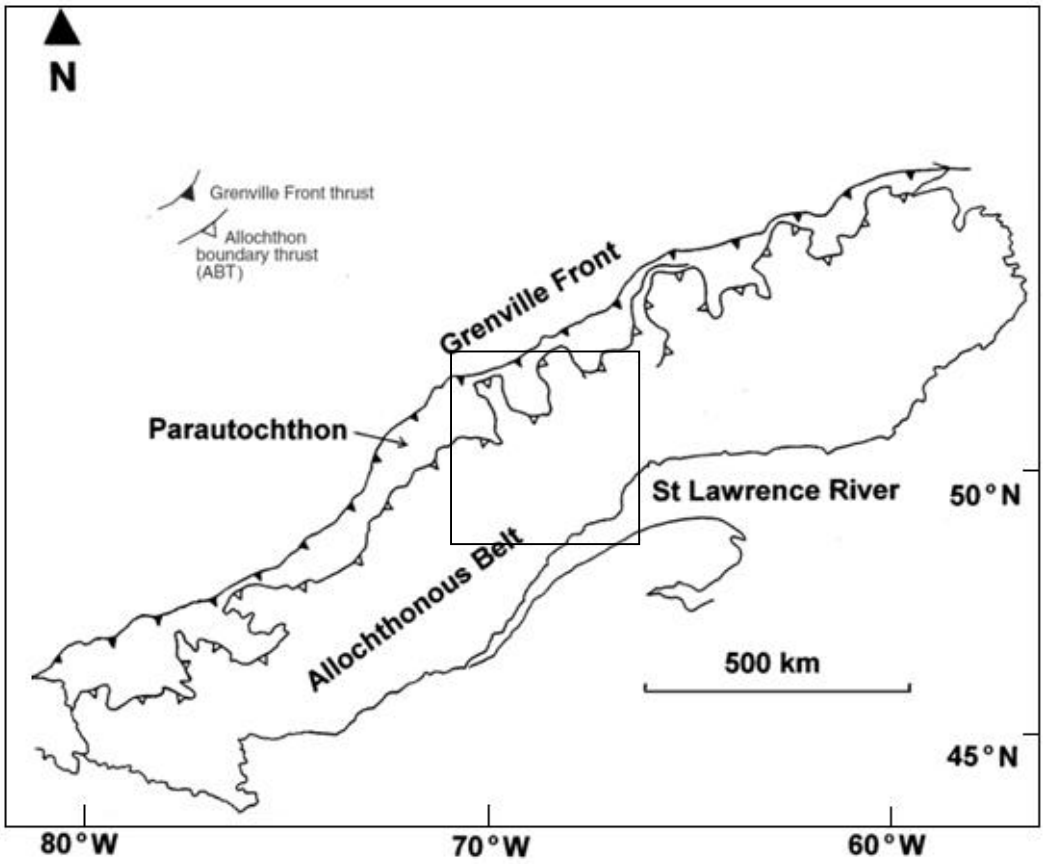

Figure 1.7: The tectonic divisions of the Grenville Province (after Rivers et al., 1989). The black box indicates the study area.

Rivers et al. (1989) defined these belts in terms of Grenvillian orogenic cycles of transposition and overprinting, each with their own tectonic boundaries: the Parautochthon in the north, the Allochthonous Polycyclic Belt in the south, and the Allonchthonous Monocyclic Belt, a restricted portion in the far east and far west (not

shown). The Parautochthon is bounded to the north by the Grenville Front and contains reworked Archean and Paleoproterozoic crust. The Allochthon Thrust Boundary (ABT) separates the Parautochthon from the largely Mesozoic Allochthonous Belt that tectonically overlays it. The present study area lies fully within the central part of the Allochthonous Polycyclic Belt (APB), characterized by multiple orogenic cycles that overprinted the belt with a high metamorphic grade of amphibolite to granulite facies (Rivers et al., 1989). However, because the present study area is smaller in scale and lies completely within the APB and deals with pre-Grenvillian tectonics, this tectonic model is not suitable for explaining the tectonics of smaller accreted terranes.

Studies of Mesoproterozoic crustal evolution must be carried out in the context of Grenvillian belts and terranes; however a detailed understanding of the pre-Grenvillian evolution of the Laurentian margin depends on the identification of accreted terranes with district ages of crustal formation. Hence, Dickin (2000) proposed that the Grenville Province could also be explained in terms of several large accreted terranes with distinct crustal formation ages: Laurentia 2.7 Ga, Barilia and Makkovikia 1.9 Ga, Labradoria 1.7 Ga, and Quebecia 1.5 Ga (Figure 1.8).

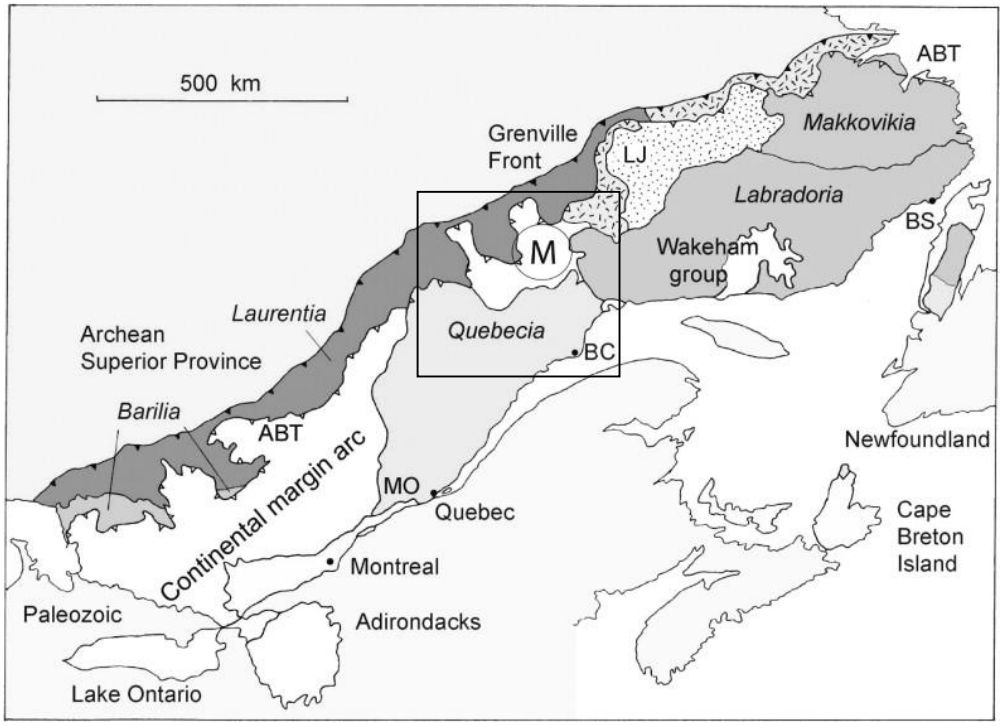

Figure 1.8: The Grenville Province and its terrane divisions based on identified crustal formation ages (Thomson et. al., 2011). M: Manicouagan Impact Crater, BC: Baie Comeau, ABT: Allochthon Boundary Thrust., LJ: Lac Joseph allochthon, largely composed of Makkovik-age sedimentary rocks. Coarse stipple: Trans-Labrador batholith. The black box indicates the study area.

1.4 The Study Area

Among the terranes proposed by Dickin (2000), the Quebecia terrane is the largest Mesoproterozoic accreted terrane, and was first identified by Dickin and Higgins (1992) as a Mesoproterozoic arc that was accreted to the Laurentian craton within 100 Ma of its formation. Figure 1.9 shows the Quebecia Terrane in relation to the Manicouagan Reservoir, the Makkovikian-age terranes to the north, and the Labradoria Terrane to the east.

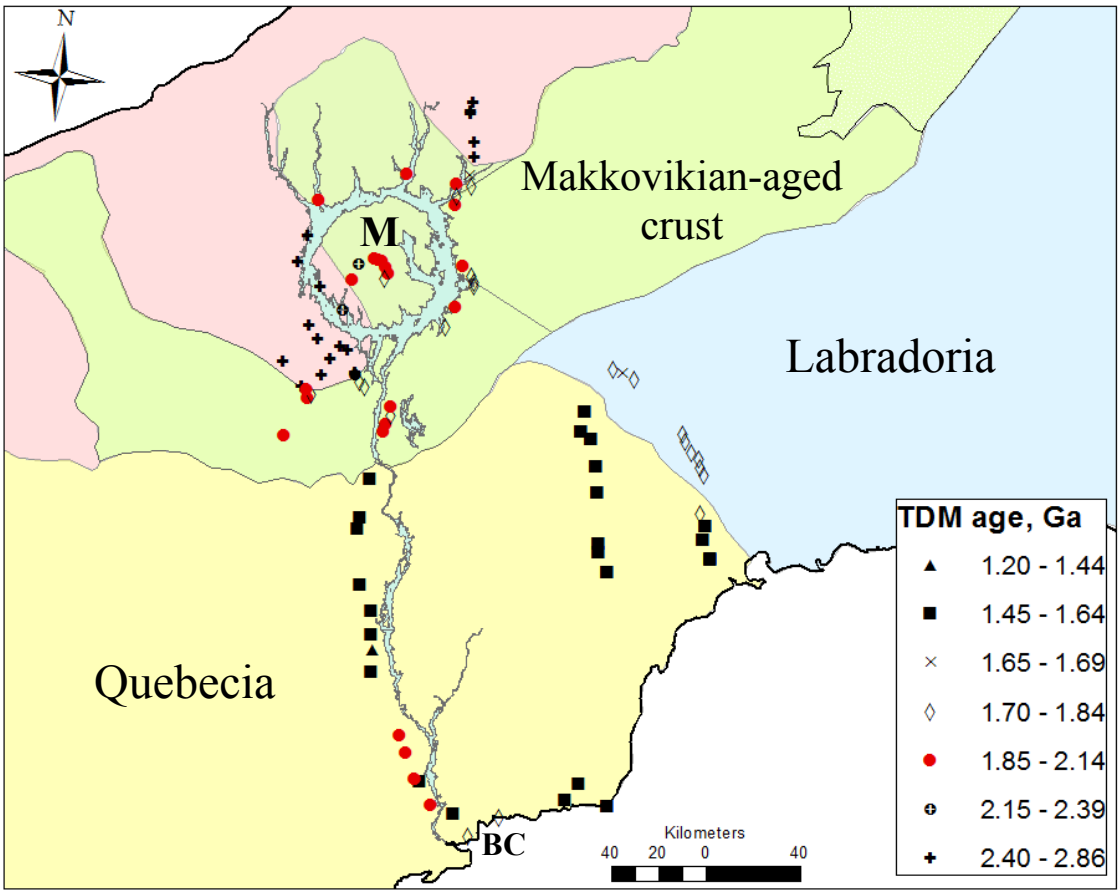

Figure 1.9: Crustal formation age map for the Quebecia Terrane (yellow) in relation to Makkovikian-age Berthe and Molson Lake terranes (green), the Labradoria Terrane (blue), Archean crust (pink) and the Manicouagan Impact Crater (M). BC=Baie Comeau. (Published data from Dickin and Higgins, 1992; Thomson et al., 2011.)

Dickin and Higgins (1992), while providing evidence for a major 1.5 Ga crustal event that would later be named the Quebecia Terrane, also identified a few samples distinct from the main sample suite yielded depleted mantle model ages of 1.7-2.0 Ga. They speculated that this may represent a separate, earlier crust forming event or a supracrustal sequence with a lithology resembling arc-derived sediments.

Hynes (2010) made a study of these enigmatic older crustal ages in the Saguenay and Baie Comeau areas of the Quebecia Terrane within Central Quebec. Hynes' study involved identifying and mapping crustal formation ages of old Paleoproterozoic

(>1.65Ga) crustal blocks that lie within the young 1.5 Ga Quebecia arc terrane. Through reconnaissance Sm-Nd isotope mapping of samples from the Saguenay and Baie Comeau areas, this study constrained the boundaries of the old crustal blocks in limited areas with Sm-Nd isotopic evidence, and proposed that the two fragments may connect to form an old crust panel running through the younger Quebecia arc. Figure 1.10 shows this model for the extended old crust panel.

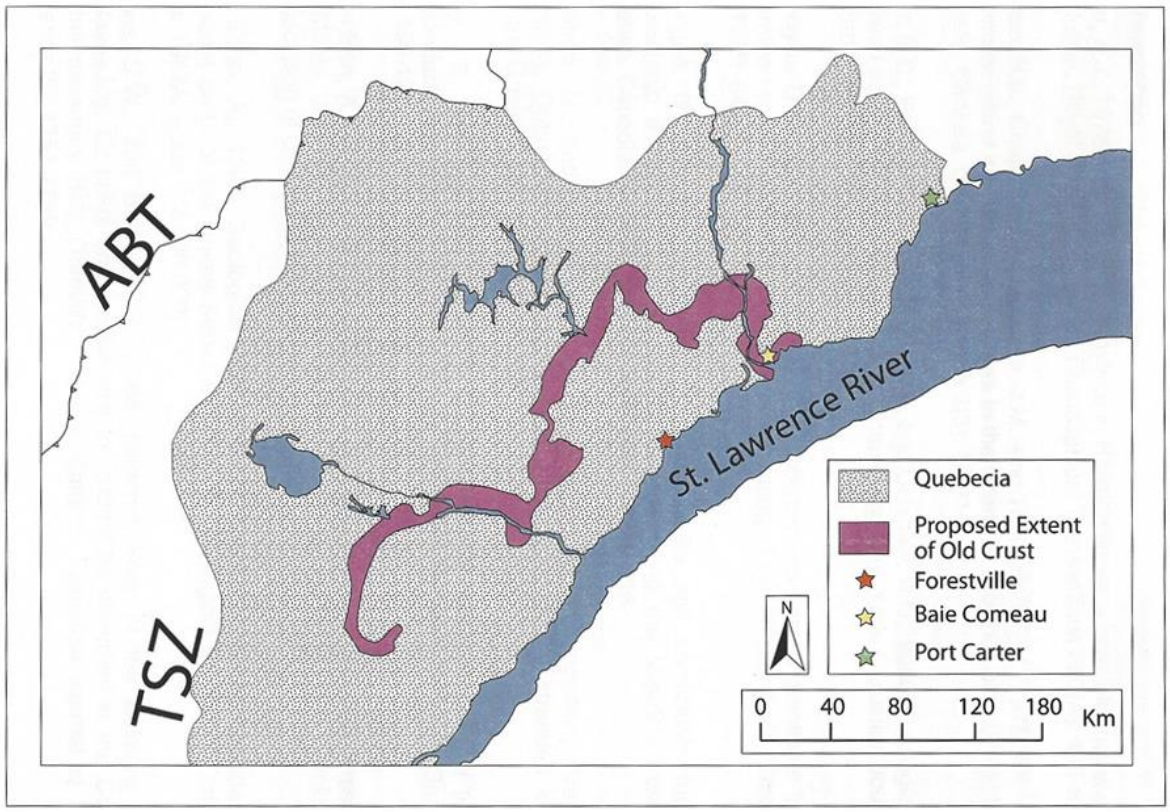

Figure 1.10: Proposed extent of old crust (purple) within the Quebecia terrane (grey) (Hynes, 2010)

Ultimately, Hynes proposed that the Quebecia Terrane may represent a tectonic setting where fragments of old lithosphere were rifted from the Laurentian margin and later incorporated into the younger arc terrane formed by subduction related magmatism;

However, more research was still needed to provide a working model of how the old fragments got to their current position within the younger Quebecia terrane, and where these fragments came from.

Samples directly north of the Quebecia Terrane may help answer the question of the original of these old fragments. The Grenville Province contains one of the largest and best preserved terrestrial impact structures, the Manicouagan Impact Structure, which is found just north of the Quebecia terrane. The Manicouagan region contains large areas of Proterozoic and Archean orthogneiss, and is subdivided into several Grenvillian lithotectonic terranes: the Gagnon terrane, Hart Jaune terrane, the Berthe Terrane, and the Manicouagan Imbricate Zone (MIZ) (Spray et al., 2010).

The Berthe Terrane is comprised of several smaller fragments that have been termed the Southern Domains. It is located southeast of the Manicouagan reservoir within the allochthonous belt (Hynes et al., 2000). Through Nd isotope analysis, the southern domains show a restricted range of Paleoproterozoic model ages from 1.7 to 2.0 Ga. A Sm-Nd isochron for samples in the Manicouagan area compared with suites from Eastern and Southern Labradoria showed that Berthe Terrane model ages fell between the distributions from eastern and southern Labrador - suggesting that the Berthe Terrane represents Makkovikian age crust that was reworked during the Labradorian orogeny (Figure 1.11).

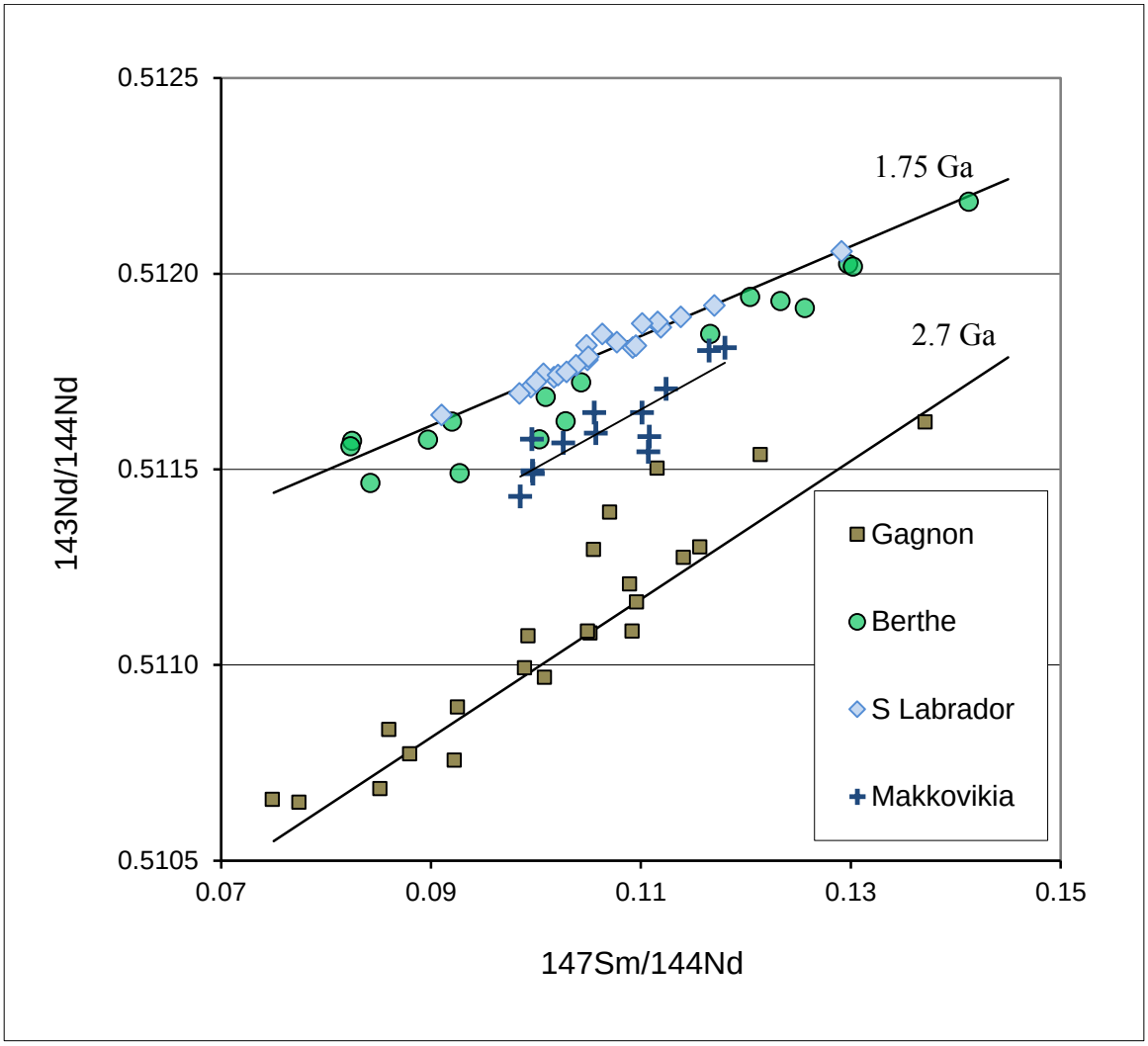

Figure 1.11: Sm-Nd isochron diagram for analyzed orthogneiss samples from the Berthe Terrane in relation to suites from Southern Labrador, Gagnon and Makkovikia (Modified from Thomson et al., 2011)

The present study utilizes Sm-Nd isotopic evidence and crustal age mapping to further investigate the northern and eastern extension of the older crustal fragments near Baie Comeau in an effort to constrain their boundaries. Ultimately, the study aims to deduce an origin for these fragments and a tectonic model of their inclusion within the Quebecia Terrane. The study focused on a series of approximately N-S transects and one

NE-SW transect within Central Quebec and the Baie Comeau area to map the boundaries of the old fragments (Figure 1.12).

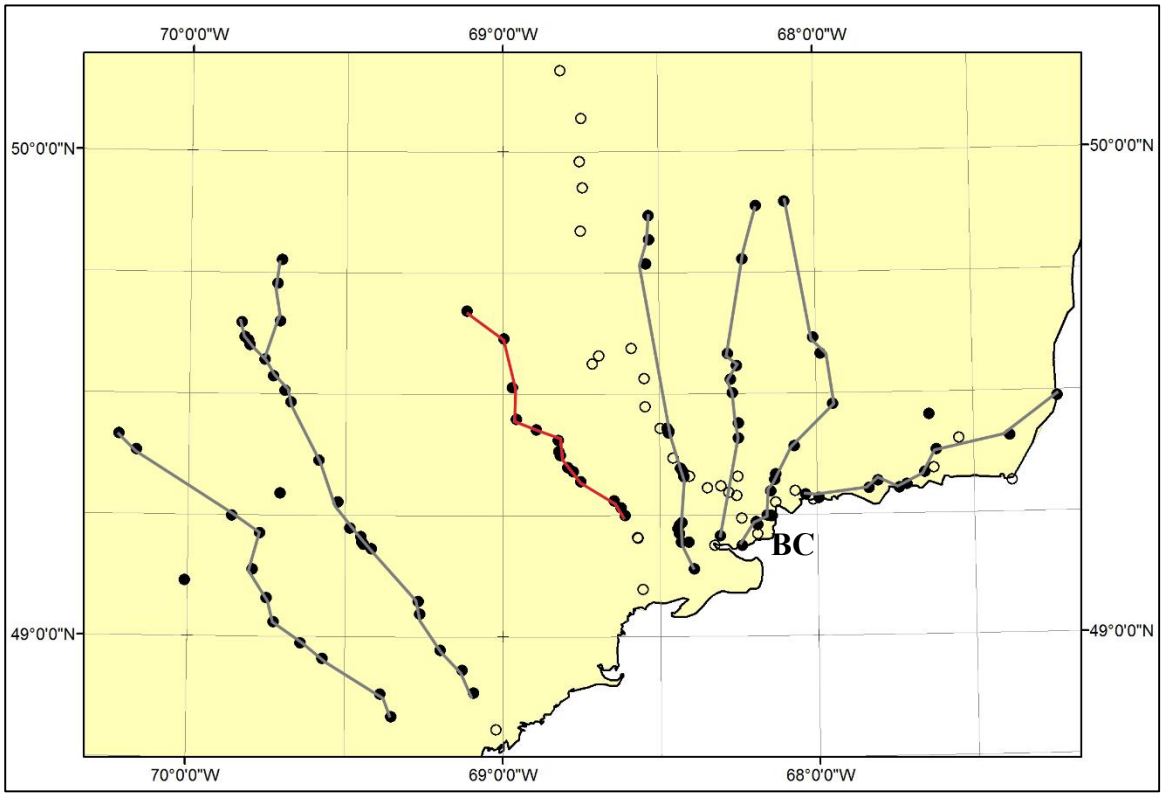

Figure 1.12: A sample transect map for the study area. BC=Baie Comeau. Red line: Baie Comeau transect for which major element geochemical data were obtained

Chapter 2 – Neodymium Model Ages

2.1 Introduction

When continental crust is extracted from the mantle, it remains buoyant relative to the mantle and creates terrestrial microcontinents that collide and form larger macrocontinents. The boundaries between these microcontinents prior to collision and accretion can be obscured by metamorphism, such as seen in the Grenville Province due to the Grenville Orogeny. Model ages can be used to identify the time at which the continental crust was extracted from the mantle, allowing the ability to date the formation of the crustal terranes and to map the boundaries between them.

The metamorphic events that affected the Grenville Province are responsible for resetting some isotope systems that could be used as dating techniques. The Samarium-Neodymium (Sm-Nd) isotope system is an ideal method for dating metamorphic rocks such as in this case because it is resistant to this resetting. The elements themselves have very similar chemical properties to each other and are relatively immobile during high grade metamorphism, erosion and igneous intrusions (Green et al., 1969; McCulloch and Wasserberg, 1978), therefore the system remains closed. Hence, the Sm-Nd dating technique can yield model crustal formation ages of the terranes as they would have been prior to metamorphism.

2.2 The Samarium-Neodymium Dating Method

Samarium has several radioactive isotopes (^{147}Sm, ^{148}Sm and ^{149}Sm) however ^{147}Sm is the most useful as it has a half-life of 106 Ga – allowing it to produce small, but measurable differences in the daughter product ^{143}Nd over millions of years (Dickin, 2005). This provides the basis of the Sm-Nd dating system. The radioactive decay law using the Sm-Nd method is expressed by the following formula:

$$\frac{143Nd}{144Nd} = \left(\frac{143Nd}{144Nd}\right)_I + \frac{147Sm}{144Nd}(e^{\lambda t} - 1)$$

Where λ = radiometric decay constant, t = age of the sample

The three ratios required to solve the age equation are the present day isotopic ratios of ^{143}Nd/^{144}Nd and ^{147}Sm/^{144}Nd, which are measured by mass spectrometry, and the initial isotopic ratio of ^{143}Nd/^{144}Nd, which must be determined before age calculation. The initial isotopic ratio can be obtained from a mantle model, which assumes that the initial ^{143}Nd/^{144}Nd ratio of the rock is equal to the ^{143}Nd/^{144}Nd ratio of the mantle at the time it is extracted (Nelson and DePaolo, 1984).

Originally, the T_{CHUR} model by DePaolo and Wasserburg (1976a, 1976b) was used to obtain the initial isotopic ratio of the mantle for the dating method. This model, shown in Figure 2.1, represents the Nd isotope ratio through earth's history. The Chondritic Uniform Reservoir (CHUR) is an established benchmark for the isotopic composition of chondrite meteorites as a representation of the evolution of solar-system bodies such as Earth (Dickin, 2005). Studies have shown that samarium and neodymium isotope ratios present in terrestrial samples are roughly similar in

abundances to chondritic meteorites (DePaolo and Wasserburg, 1976a, 1976b), leading to the currently accepted theory that mantle composition was derived from the same source as chondrite samples; thus, Earth accreted from material with chondritic signatures.

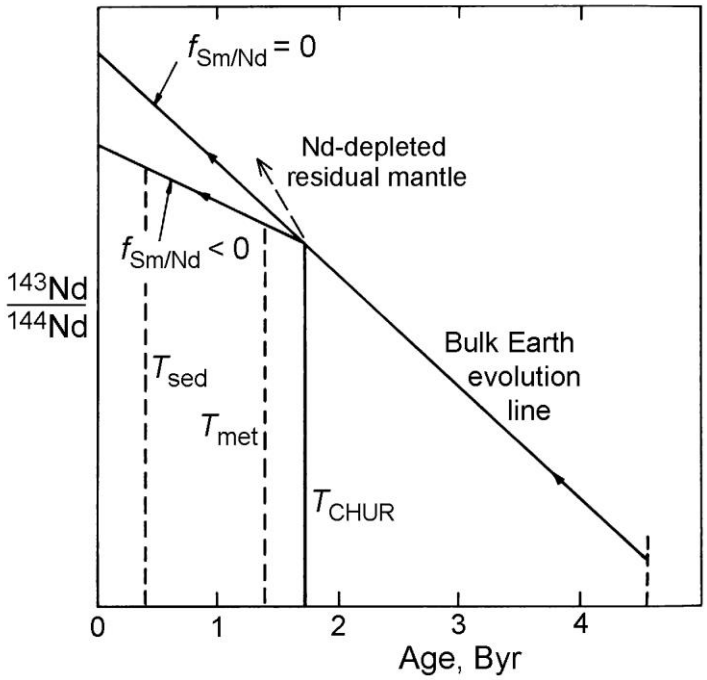

Figure 2.1: Nd isotope evolution diagram; T_{met} = age of metamorphic event; T_{sed} = age of erosion event; f = fractionation of sample Sm/Nd (Dickin, 2005)

In DePaolo and Wasserburg's 1976a study, a new notion was also developed by normalizing all initial $^{143}Nd/^{144}Nd$ isotopic ratios to CHUR to remove any effects of the slight fractionation that occurs between Sm and Nd, and for easier comparison between of different aged samples:

$$\varepsilon Nd(t) = \left[\frac{\left(\frac{143Nd}{144Nd}\right) sample\ (t)}{\left(\frac{143Nd}{144Nd}\right) CHUR\ (t)} - 1\right] x\ 10^4$$

DePaolo and Wasserburg (1976b) proposed that if this model is correct, and the CHUR evolution line accurately identifies the initial Nd isotope ratio of the mantle through time, then any measurement of Sm-Nd ratios in a crustal rock can be compared to the model and yield a model age for the formation of that rock, as long as there is sufficient isotope fractionation during crustal extraction from the mantle. This model is represented by the following formula:

$$T_{CHUR} = \frac{1}{\lambda}\ln\left[1 + \frac{(\frac{143Nd}{144\,Nd})sample - (\frac{143Nd}{144Nd})CHUR}{(\frac{147Sm}{144\,Nd})sample - (\frac{147Sm}{144Nd})CHUR}\right]$$

Although Archean plutons fit the CHUR line, Mid-ocean ridge basalts (MORB) samples lay +7 to +12 ε units above the CHUR line (Figure 2.2) – leaving a gap between Archean CHUR data and the depleted MORB source (indicated by elevated Sm/Nd ratios) due to a lack of Proterozoic data.

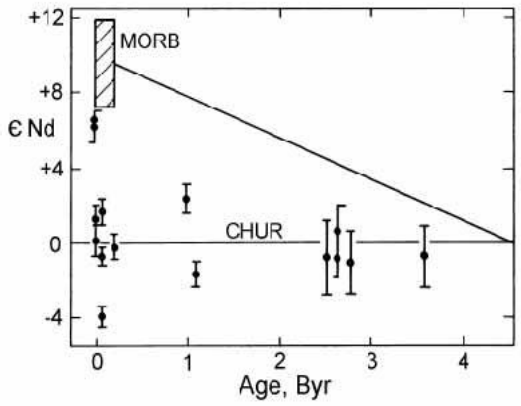

Figure 2.2: Diagram of Nd isotope evolution against time, showing terrestrial sample deviations from the CHUR line in ε units. (DePaolo and Wasserburg, 1976b)

DePaolo (1981) recognized that Archean samples that fell within error of the CHUR line could actually lie on a curved corresponding to the progressive depletion of the mantle in light rare earth elements (LREE), representing a depleted-mantle evolution

line. To test this, DePaolo (1981) studied the Proterozoic basement from the Colorado Front Range and presented the initial $^{143}Nd/^{144}Nd$ ratios of the samples in Figure 2.3.

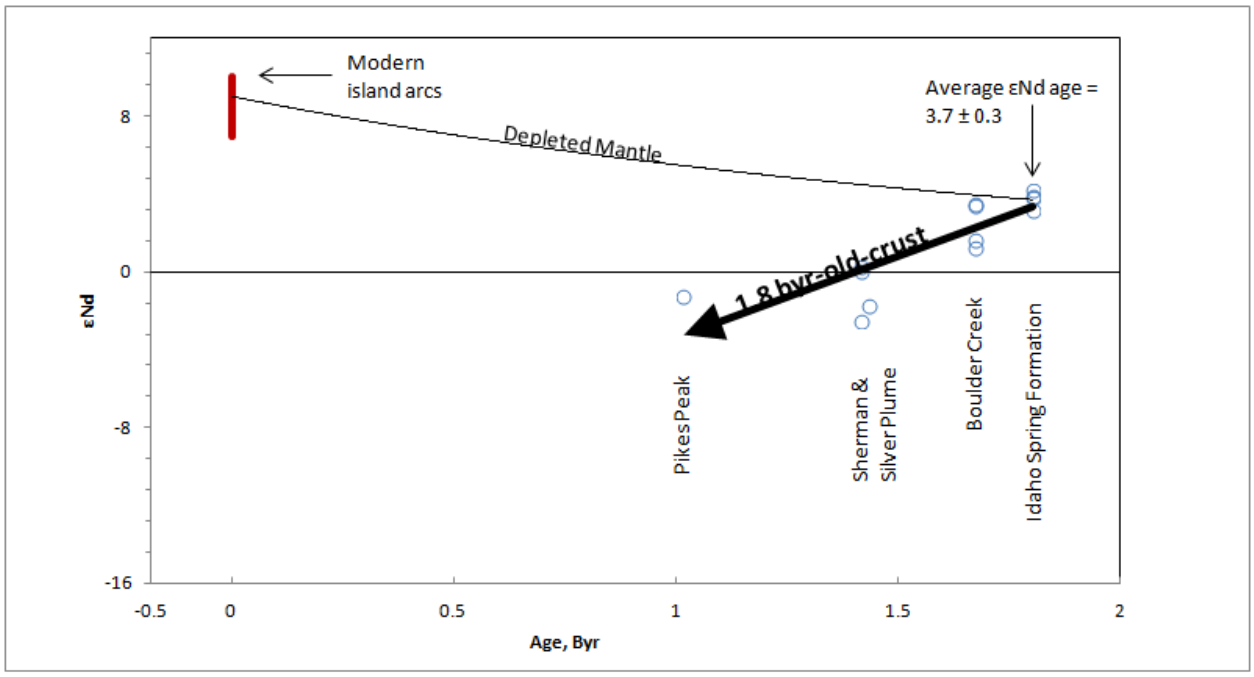

Figure 2.3: Plot of ε Nd against time, showing the Colorado Front Range data relative to a depleted-mantle evolution. (After DePaolo, 1981)

DePaolo (1981) fitted a quadratic curve to the data, representing the Nd isotope evolution of a depleted reservoir that was a source for subduction-related magmatism. The curve begins on the CHUR evolution line in the early Archean, but evolves steadily to the present day. The composition of the depleted reservoir, relative to CHUR, is given as:

$$\varepsilon Nd(T) = 0.25T^2 - 3T + 8.5$$

Sm-Nd model ages calculated using the depleted mantle curve are denoted T_{DM}, and have been shown empirically to yield more accurate indications of crustal formation ages than T_{CHUR} ages for studies of continental evolution (DePaolo, 1981).

Mass spectrometry was utilized at McMaster University in Hamilton to analyze the samples for their Sm-Nd isotope signatures in order to establish model ages. Please refer to Appendix A for detailed laboratory techniques.

Chapter 3 – Results

3.1 Nd Isotope Data

The current study aimed to investigate the extent of the old Paleoproterozoic crustal block within the younger Mesoproterozoic Quebecia terrane, as well as provide evidence for its origin and tectonic history. The results of the present study, along with preciously published data, have been compiled into three tables (See Appendix B). Table B-1 shows model age results that fall within the age range corresponding to the Quebecia Terrane (1.46-1.64 Ga) as defined by Dickin (2000), Table B-2 gives the results for model ages that are Labradorian to Makkovikian (1.7-2.0 Ga), while Table B-3 contains intermediate model age results that area attributed to Nd mixing at the boundaries between old and young blocks (1.65-1.69 Ga).

Samples which returned model ages which seemed anomalous were duplicated and reanalysed to check the results, either by complete redissolution or a duplicate analysis for $^{143}Nd/^{144}Nd$ ratio. Samples indicated by a '*' were taken from Hynes (2010), '**' from Dickin and Higgins (1992) and '***' from Dickin (2000). After the crustal formation ages were calculated, they were plotted in ArcGIS (Figure 3.1). The Paleoproterozoic ages appear to form a sinusoidal pattern in the Baie Comeau (BC) area in Central Quebec – suggesting they could have originated as a single elongated block extending through the Mesoproterozoic Quebecia Terrane.

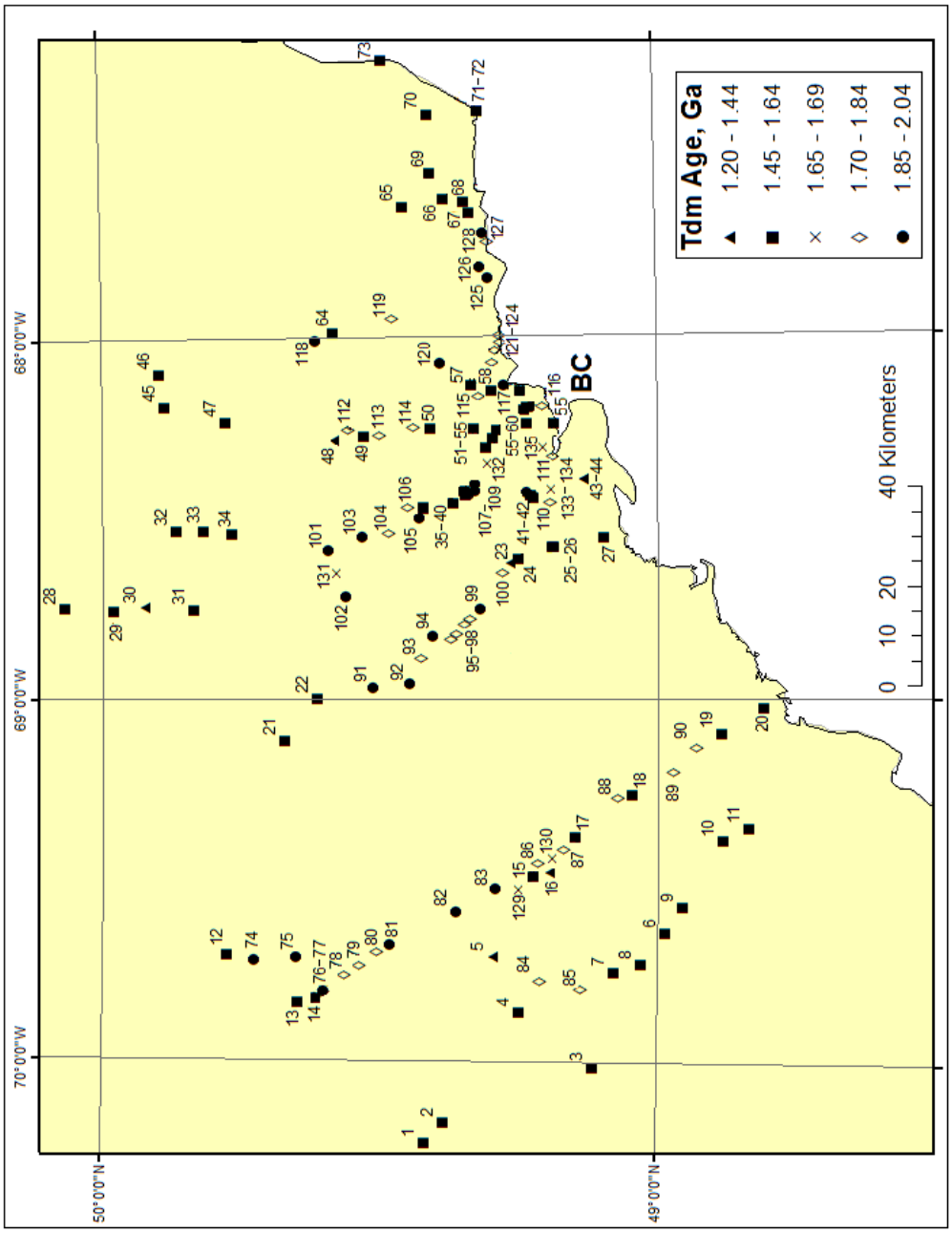

Figure 3.1: A numbered map of all the sample data found in tables B-1, B-2 and B-3.

A Sm-Nd isochron diagram was generated using the age categories in the above tables, along with several published reference suites (Figure 3.2).

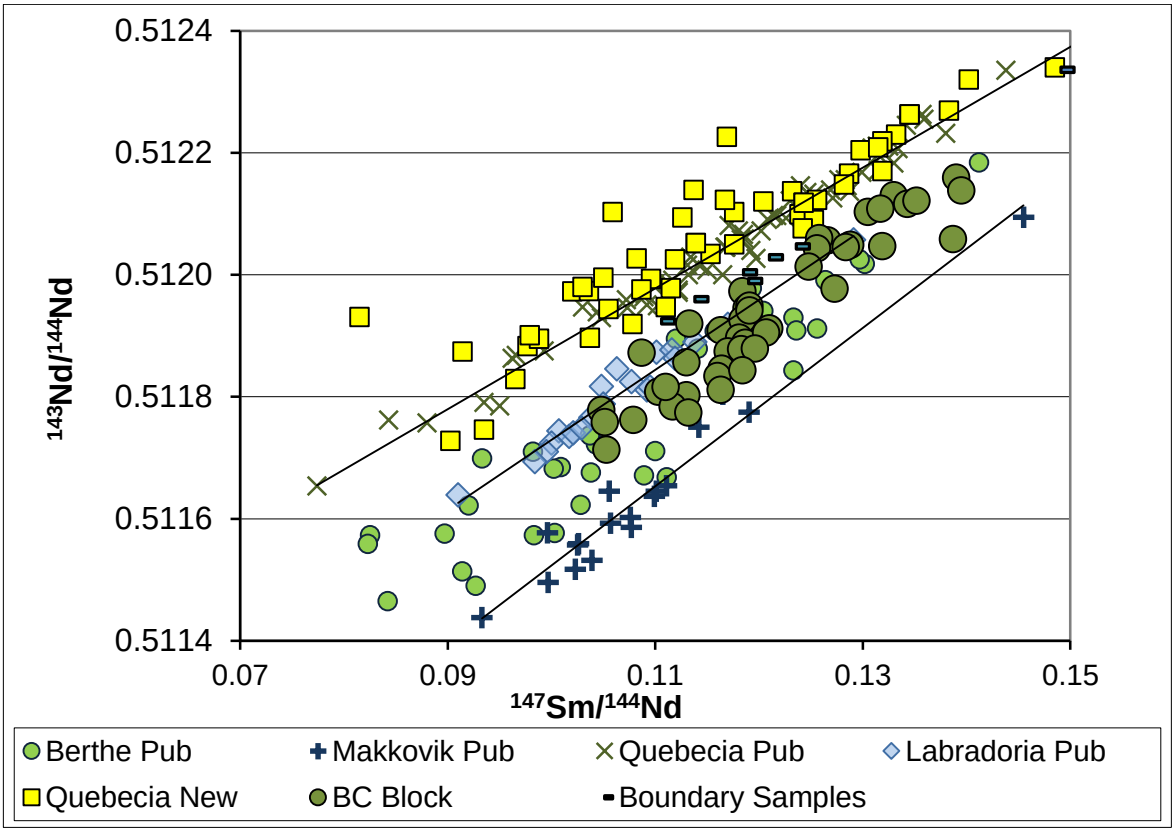

Figure 3.2: An isochron diagram comparing published data for the Quebecia Terrane, Makkovik province, Labradoria, and the Berthe Terrane with the current study. (Published data from Dickin, 2000; Hynes, 2010; Kerr and Fryer, 1994; Ketchum et al., 2002; Thomson et al., 2011).

New Quebecia-aged samples plot close to the published suite for Quebecia. In contrast, rocks from the Paleoproterozoic Baie Comeau block fall between the reference lines for the juvenile Labradoria Terrane and the Makkovik Province. This suggests the BC Block may contain a mixture of Nd with Makkovikian and Labradorian ages.

The Berthe Terrane exhibits a similar mixing pattern between Labradorian and Makkovikian aged crustal material, suggesting that a Laurentian source similar to the Berthe Terrane may have been detached to form the old block within Quebecia. As shown in Figure 1 by the red circles, the Berthe Terrane directly north of Quebecia has already

been attributed to the intrusion of Labradorian magmas into an older Makkovikian terrane.

To further examine the possible origins of the Baie Comeau block, it is compared with T_{dm} ages of the surrounding terranes in Figure 3.3, which presents a series of histograms illustrating the frequency of model ages for previous studies in Labradoria, Makkovikia, Quebecia and the Berthe Terrane, along with the current study.

The data distribution for the new Quebecia samples shows a peak at 1.55 Ga, which accurately reflects the published Quebecia peak value. In contrast, the BC Block shows a distribution ranging from 1.7-2 Ga, with peaks at 1.75 Ga and 1.85 Ga, illustrating a similar distribution to the Berthe Terrane but slightly shifted downward in age. This suggests that the Berthe Terrane and the BC block contain slightly different mixtures of Makkovik and Labradoria components. This may reflect reworking of Makkovikian crust in a Labradorian-age continental margin arc, as proposed for SE Labrador (Moumblow, 2014). The fact that the BC Block contains a slightly larger fraction of Labradorian Nd suggests that it may represent a slightly more out-board segment of this continental margin than the crust presently preserved in the Berthe Terrane.

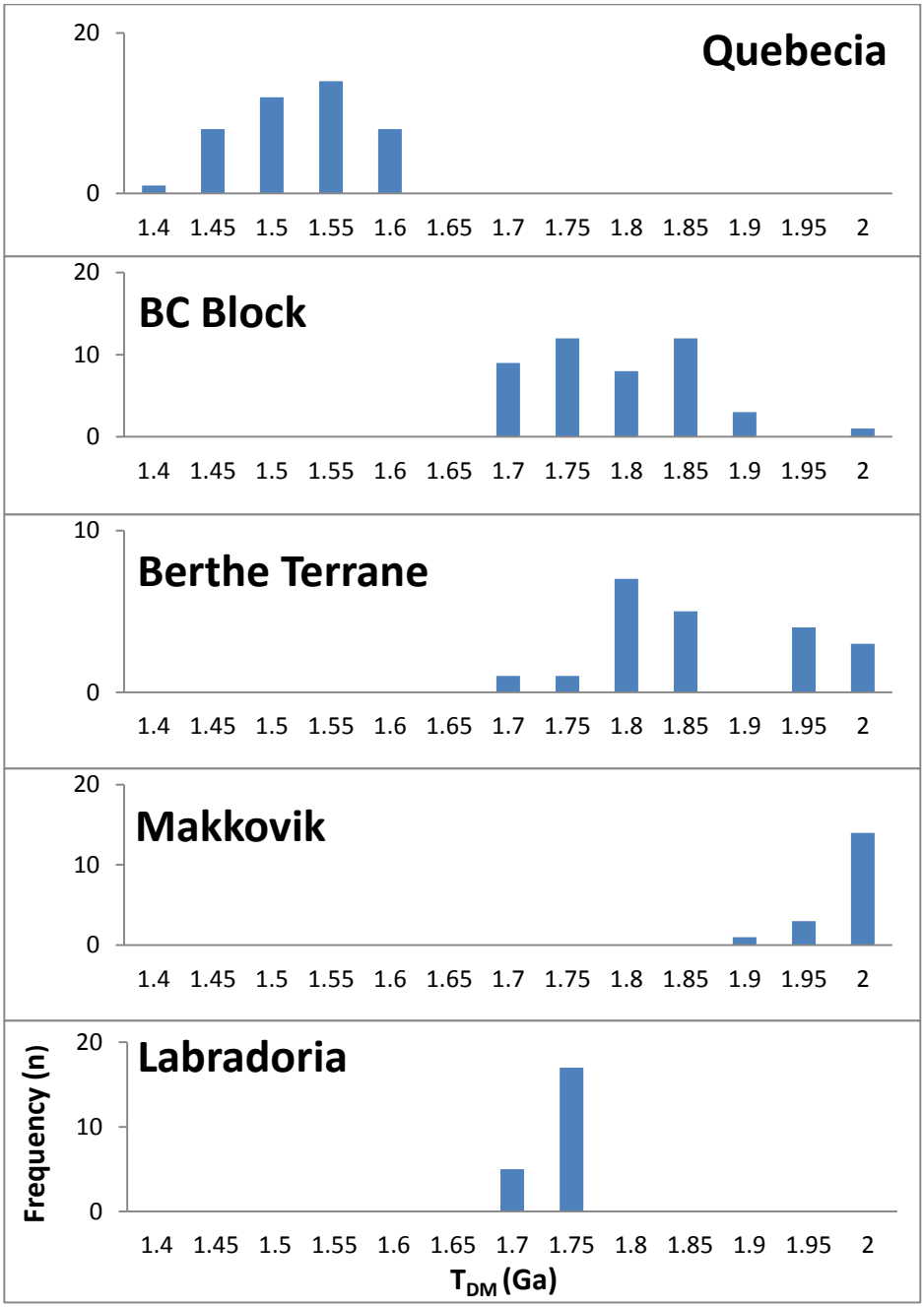

Figure 3.3: Distribution of T_{DM} age for the BC block compared with the surrounding terranes of Quebecia, Berthe, Labradoria, Makkovik. (Published data from Hynes, 2010; Kerr and Fryer, 1994; Ketchum et al., 2002; Thomson et al., 2011.)

3.2 Geochemical Analysis

In order to compare the petrology of the BC block with the Quebecia Terrane, samples from the principal transect west of BC were analyzed geochemically. These results are shown in Table 3.4 (See Appendix B). The results were compared with published data to produce a series of geochemical plots shown in Figure 3.4, 3.5, 3.6, 3.7 and 3.8. Published data from the Kohistan Arc (Jagoutz et al., 2009) was included to represent an oceanic arc for comparison.

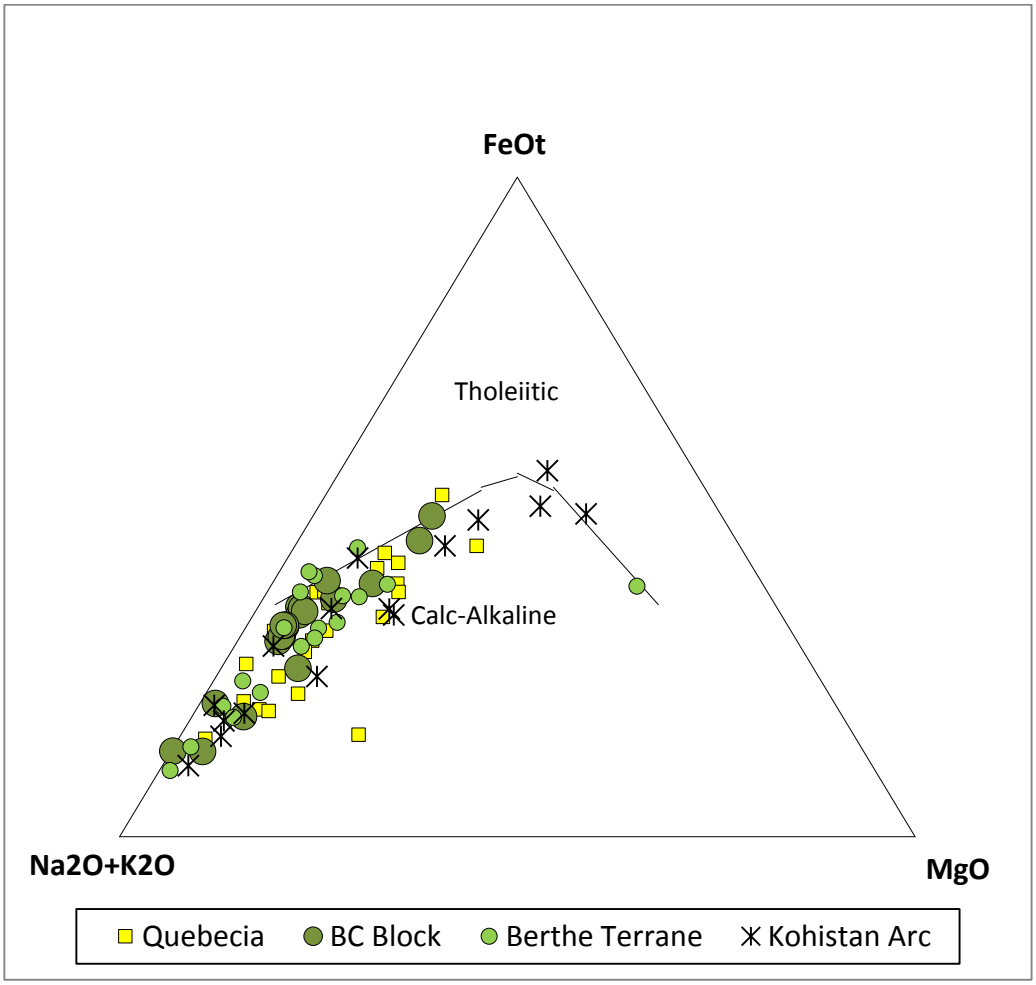

Figure 3.4: AFM Ternary diagram comparing published Quebecia, Berthe Terrane and Kohistan Arc data with the BC Block (Published data from Dickin and Higgins, 1992; Thomson et al., 2011; Jagoutz et al., 2009; Kimmerle, 2014; and Slaman, 2013).

Figure 3.4 shows an AFM Ternary Diagram that was generated using the relative proportions of oxides $Na_2O + K_2O$ (A), FeO total (F), and MgO (M). The majority of the samples lie within the calc-alkaline section of the AFM Ternary diagram, confirming that all of the samples are arc related. The data were then plotted on a Q (quartz) and P (plagioclase) petrochemical diagram to further classify granitoid rocks using their whole rock chemical composition (Figure 3.5).

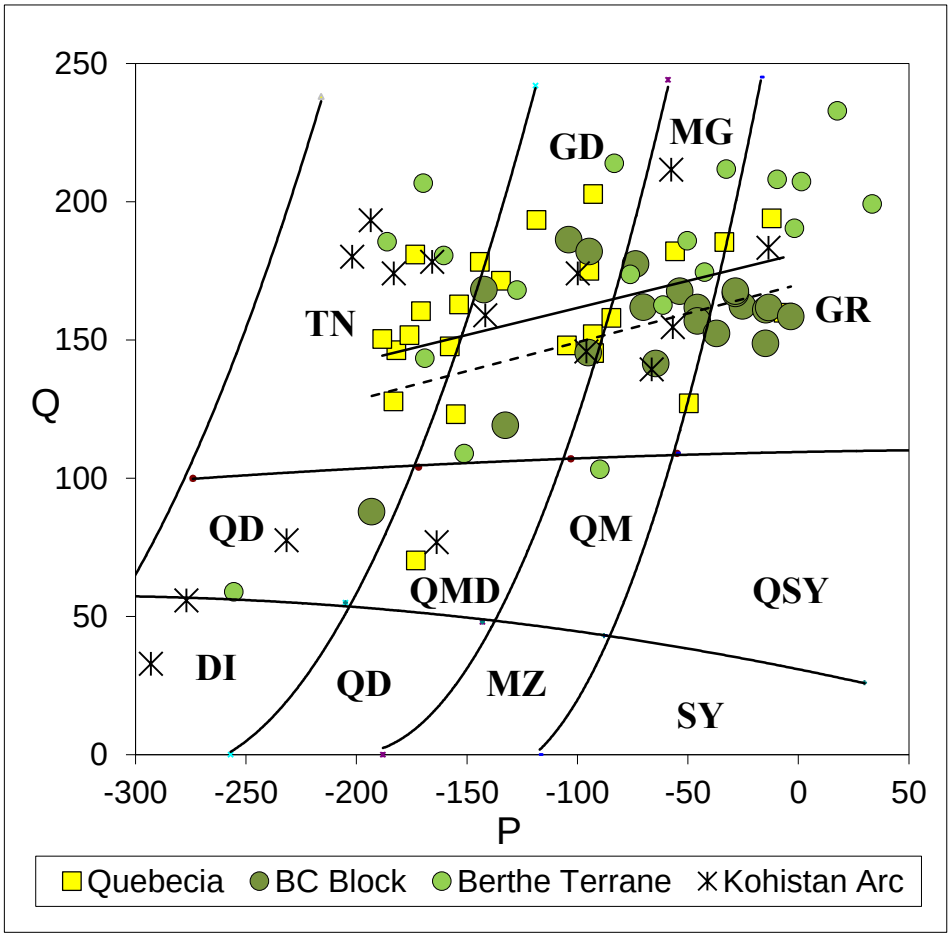

Figure 3.5: Q-P Petrochemical diagram after Debon and LeFort (1983) comparing published Quebecia, Berthe Terrane and Kohistan Arc data with the BC Block. Solid line: Quebecia trend line, dashed line: BC Block trend line (Published data from Dickin and Higgins, 1992; Thomson et al., 2011; Jagoutz et al., 2009; Kimmerle, 2014; and Slaman, 2013).

The Kohistan Arc, representing a mature oceanic arc, trends along the left side of the diagram, spanning from diorite to granodiorite. The Mesoproterozoic Quebecia samples plot predominantly in the upper region of the plot with a concentration in the tonalite and granodiorite fields (solid trend line). In contrast, samples from the BC Block plot lower and to the right (dashed trend line) indicating a lower silica, more alkaline suite.

A TAS diagram (Le Bas et al., 1986) was generated to compare silica saturation between the different sample suites (Figure 3.6). In this diagram, the Kohistan Arc suite spans mostly the entire silica oversaturated bottom region, whereas the BC Block has a tighter cluster around the boundary between oversaturated and saturated, with concentrations in the dacite (O3) and rhyolite fields. The Berthe Terrane and Quebecia Terrane suites show a similar distribution within dacite and rhyolite fields but are more scattered within the oversaturated region. This diagram is again showing that the BC block (dashed trend line) is more alkaline and less oversaturated with silica than the Kohistan arc and the Quebecia terrane (solid trend line).

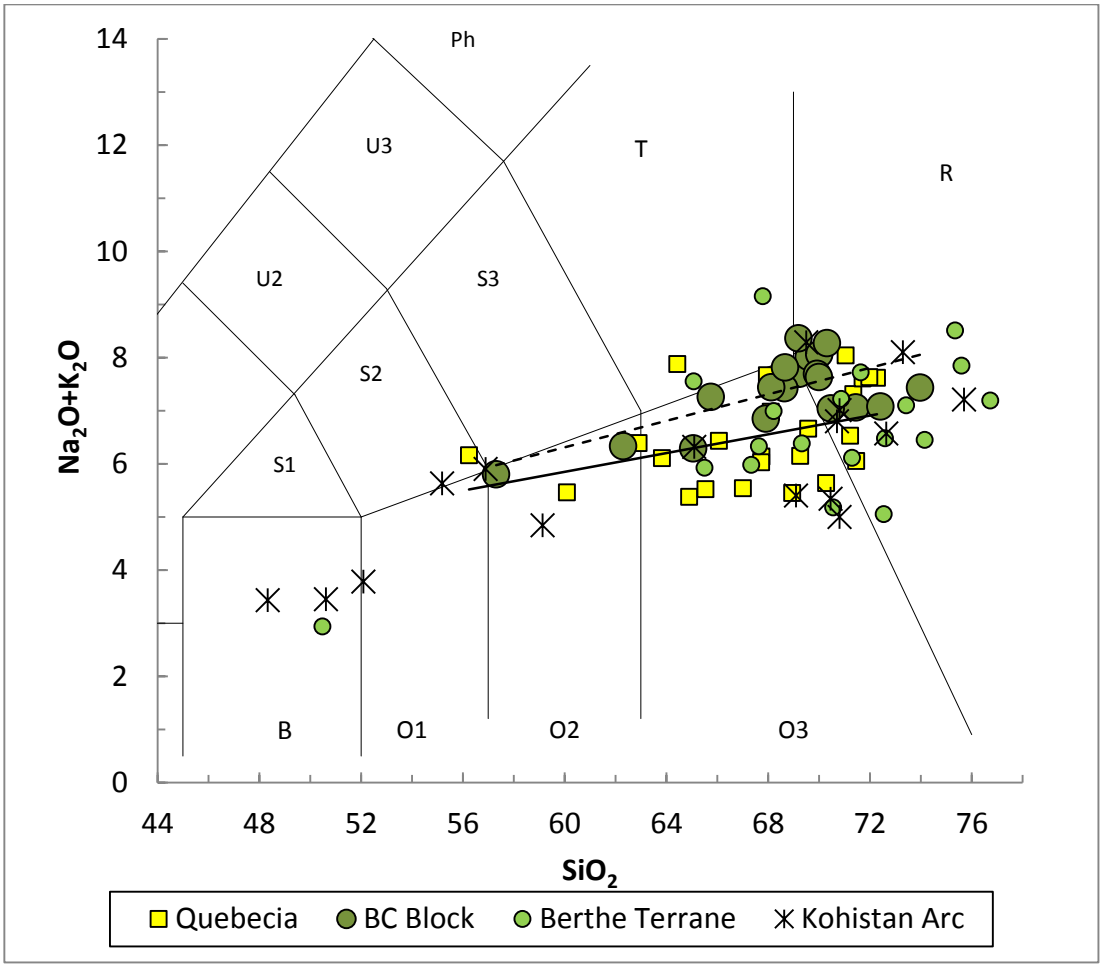

Figure 3.6: A TAS diagram comparing total alkalis and SiO_2 (Le Bas et al., 1986). U2, U3: Generally Silica Under saturated; Ph: Phonolite; S1, S2, S3: Generally Silica-Saturated; T: Trachyte or Trachydacite; B: Basalt; O1 (Basaltic andesite), O2 (Andesite), O3 (dacite): Generally Silica Oversaturated. Solid line: Quebecia trend line, dashed line: BC Block trend line (Published data from Dickin and Higgins, 1992; Thomson et al., 2011; Jagoutz et al., 2009; Kimmerle, 2014; and Slaman, 2013).

In order to further differentiate between tectono-magmatic environments, a R_1-R_2 diagram was generated to compare the calculated chemical limits of the sample suites (Figure 3.7).

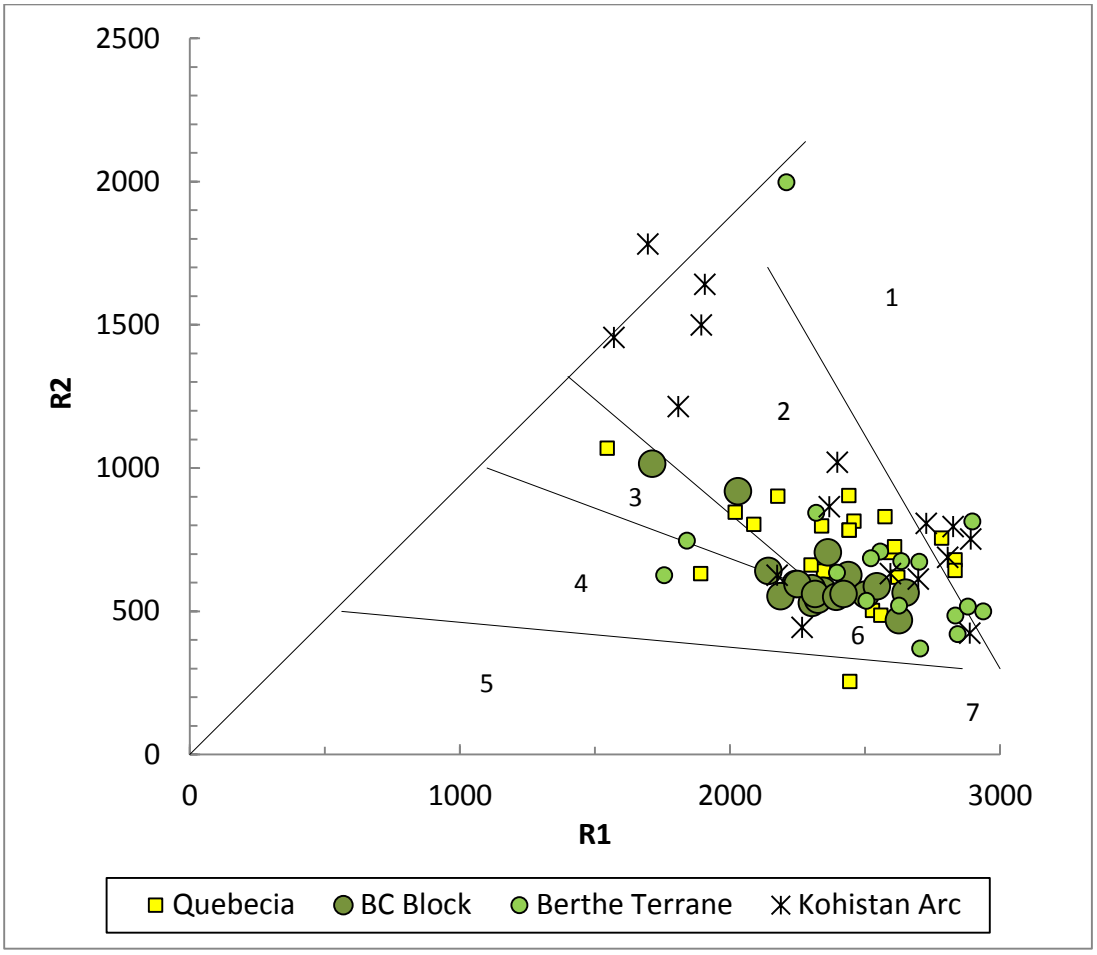

Figure 3.7: R_1-R_2 diagram: A geochemical classification of granitic rocks by Batchelor and Bowden (1985). R_1: 4Si – 11(Na+K) – 2(Fe + Ti), R_2: 6Ca +2Mg + Al. Region 1: Mantle fractionates, Region 2: Pre-plate collision, Region 3: post-collision uplift, Region 4: late orogenic, Region 5: Anorogenic, Region 6: Syn-collisional, Region 7: Post orogenic. (Published data from Dickin and Higgins, 1992; Thomson et al., 2011; Jagoutz et al., 2009; Kimmerle, 2014; and Slaman, 2013).

In the R_1-R_2 diagram, majority of the Kohistan Arc samples plot within Region 1 and 2, corresponding to mantle fractionate and pre-plate collision. The Quebecia samples plot similarly within Region 2. In contrast, the BC Block and Berthe Terrane mainly lay within Region 4 and 6, corresponding to late orogenic and syn-collisional activity. This suggests the BC block and Berthe Terrane are more mature, continental arcs in

comparison to the more primitive, oceanic arc setting Kohistan Arc and Quebecia Terrane.

Lastly, potassium oxide was plotted against zirconium concentration to further show the distribution of alkalinity (Figure 3.8). Trend lines for the BC Block (dashed line) and Quebecia (solid line) were also plotted.

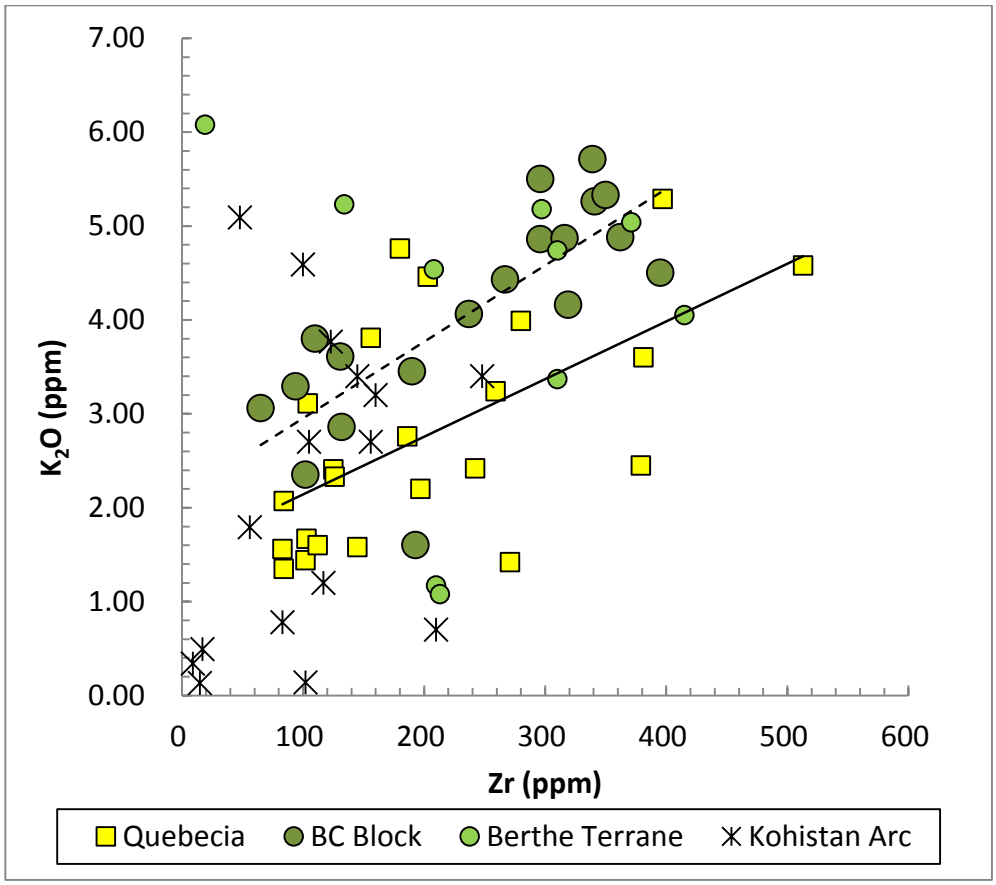

Figure 3.8: Petrochemical chart comparing potassium oxide (K_2O) and zirconium (Zr). (Published data from Dickin and Higgins, 1992; Thomson et al., 2011; Jagoutz et al., 2009; Kimmerle, 2014; and Slaman, 2013).

As shown by the trend lines, the BC Block plots higher in K_2O, indicating it is a more alkaline suite. In contrast, the Quebecia samples plot lower in K_2O, suggesting they are less alkaline, representing a juvenile arc similar to Kohistan.

3.3: Distance vs. T_{dm} Transects

The BC Transect shown in Figure 1.12 (red line) was further graphically analyzed by plotting the sample ages with the N-S distance relative to the farthest northern point above the BC Block boundary (Figure 3.9). For comparison, a transect from the Berthe Terrane and Quebecia near Manicouagan were also plotted.

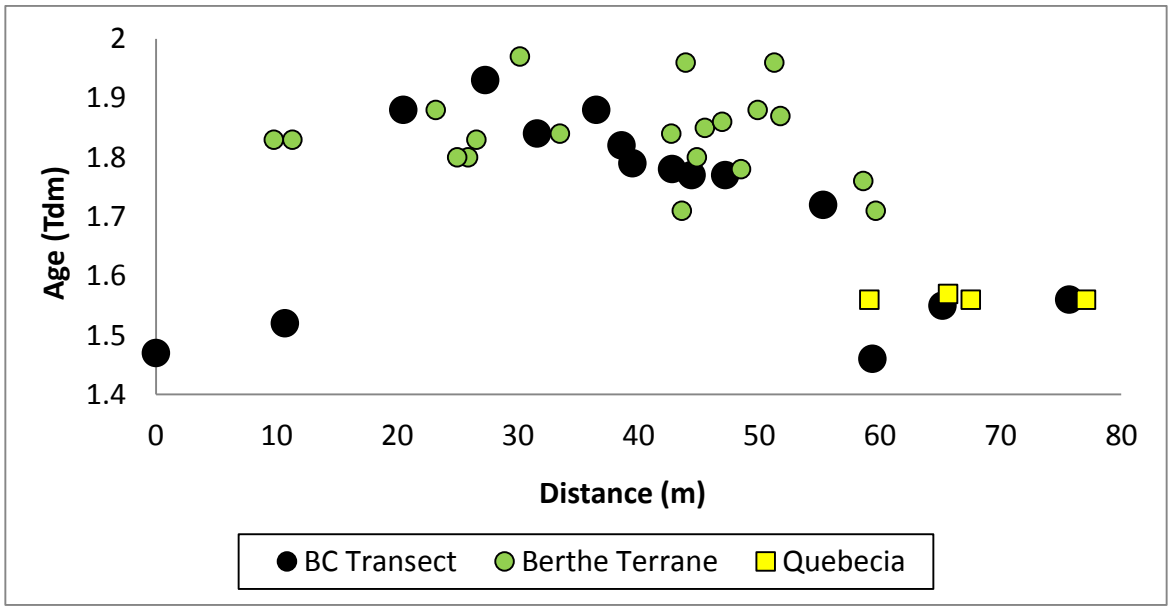

Figure 3.9: Model age/distance transect graph for the BC Transect (Published data from Thomson et al., 2011; Dickin and Higgins, 1992).

The BC Transect in Figure 3.9 begins north of the proposed old block boundary (m=0) where the samples are Mesoproterozoic in age (1.5-1.55 Ga) which represent Quebecia. As the transect moves into the old block boundary, the plotted samples yield

much older ages (1.7-1.9 Ga) and have been correlated with a Berthe Terrane transect (green circles) to show the similarity in age on the graph. As the BC transect moves out of the proposed old block boundary, the samples are again younger and correlate with well with a small Quebecia transect (yellow squares).

Chapter 4: Discussion

4.1 Discussion of Results

The present study has mapped crustal formation ages of the Quebecia Terrane (1.52 ± 0.09 Ga) in contrast to the Paleoproterozoic block identified (1.81 ± 0.07 Ga). An interpolation map was created to highlight the Paleoproterozoic ages and ultimately, determine a shape for this old Baie Comeau panel extending through the Quebecia Terrane (Figure 4.1).

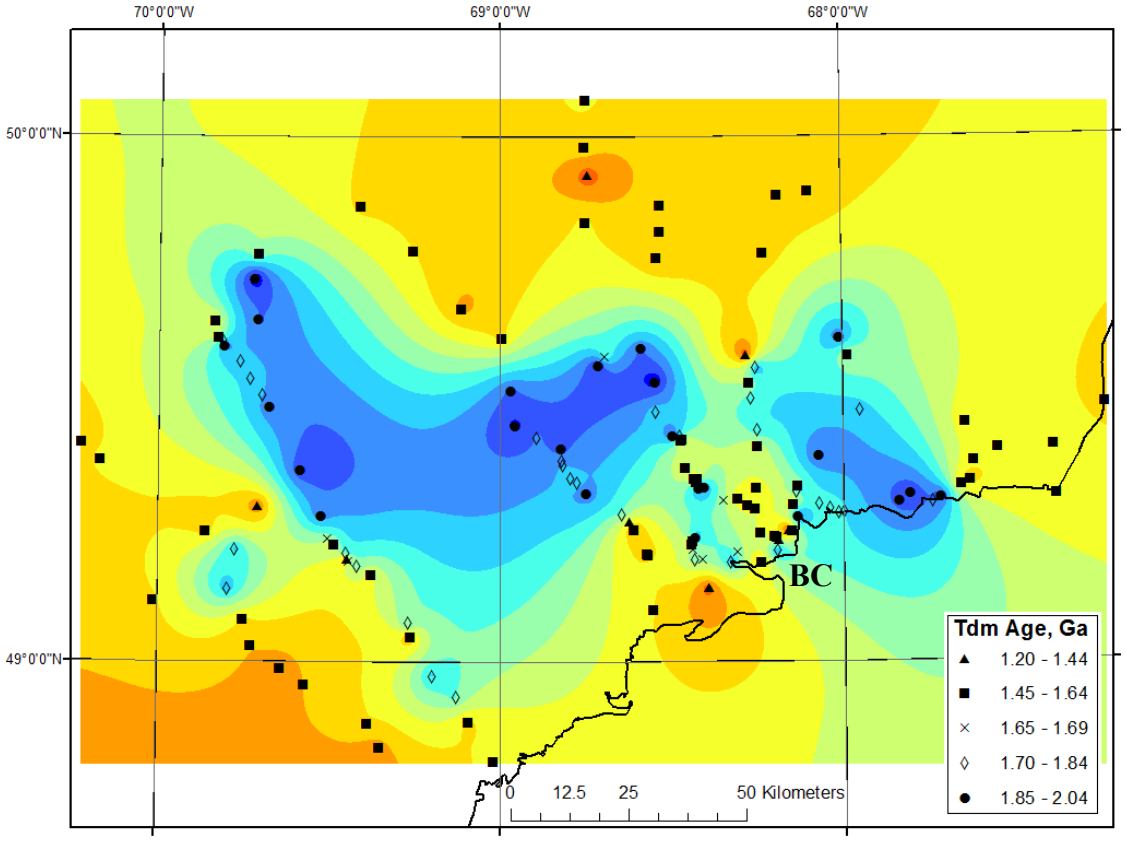

Figure 4.1: An inverse distance weighted interpolation of the Baie Comeau (BC) area in Central Quebec; Highlighting a possible shape for the Paleoproterozoic panel extending through the Quebecia Terrane.

As shown in Figure 4.1, the interpolation succeeded in highlighting the older Paleoproterozoic ages within the Baie Comeau area (blue) as two or three broken panels, as opposed to Hynes' (2010) one large panel (Figure 1.10). There was no solid evidence to link the Baie Comeau segments to the Saguenay, however as this model shows two or three separate blocks, it is not inconceivable that they are still from the same tectonic event and were broken due to Grenville metamorphism.

To further validate the highlighted panel from Figure 4.1, the regional geology was incorporated into ArcGIS along with the interpolation. Figure 4.2 shows the regional geology (obtained from *Energie et Ressources naturelles, Québec*) overlain by possible BC block fragments drawn in an effort to agree with the both the interpolation and the mapped geology. By comparing the two figures, it can be seen that there are strong NS geologic features that cut across the interpolation in Figure 4.1 (shown by the yellow star in Figure 4.2), suggesting that there is a break in the BC panel and it is instead divided into several separate segments that take the form of a mega-boudins. Since there are no roads within this area for sample collection, we rely on the geologic mapping for the shape of the BC fragment in that area.

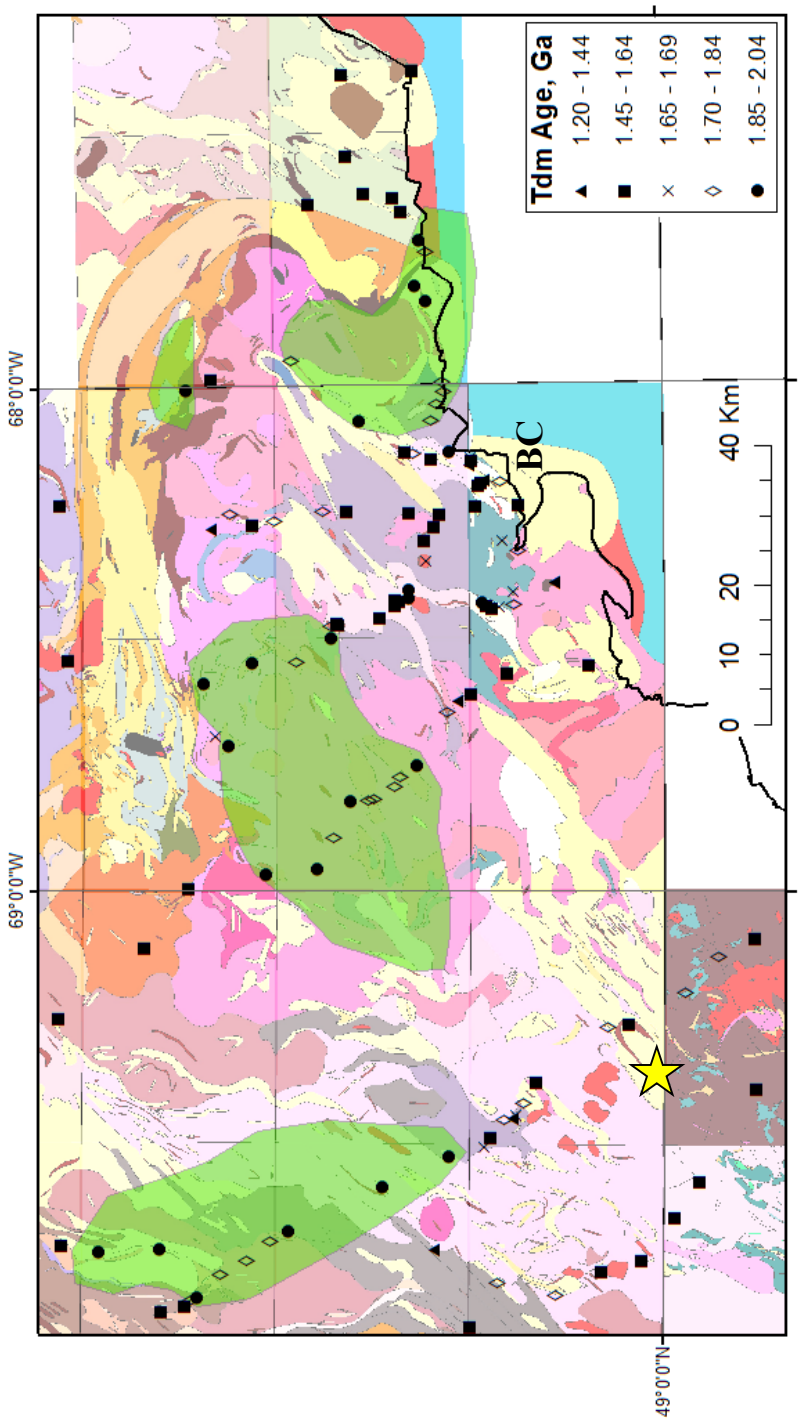

Figure 4.2: Possible configuration of the BC block fragments overlaying the regional geology. Pinks and greys: granitoid orthogneiss, oranges: anorthosite, yellow: mainly paragneiss. Yellow star indicates areas of NS linear features (Geologic maps from *Energie et Ressources naturelles, Québec*) BC: Baie Comeau.

By comparing the Sm-Nd signatures from this study with previous published work in Chapter 3, it is shown that this old block exhibits a similar mixed source signature to the Berthe Terrane. The old block may have been detached from the Paleoproterozoic margin of Laurentia and reaccreted between two blocks of the Quebecia Terrane. This leads to a model involving a division of Quebecia into separate north and south accreting terranes. The exact mechanics of this event are still unclear, however, comparison with a modern analogue may shed some light on the process.

The tectonic evolution of the Grenville Province has many similarities to that of the Sumatra region in Southeast Asia. Southeast Asia, like Laurentia, is a complex assembly of crustal terranes and volcanic arcs with tectonic boundaries between them. It is possible that the tectonic history of the old crustal block identified within the Quebecia arc may be analogous to that of West Sumatra.

4.2 Southeast Asia: A Modern Analogue

Similar to the older BC block presented in the current study, the question of how West Sumatra was transported to its current position between two younger terranes was a problem when trying to reconstruct the plate tectonics of the Sumatra region. However, being of Phanerozoic age, the tectonic history of SE Asia has been reconstructed based on floral and faunal data, as well as its deformational history. Despite the absence of these data in the Grenville Province due to its older age, the mechanism behind the

transportation of West Sumatra can be used an analogue to explain the origin of the older crustal fragments contained within Quebecia.

As shown in Figure 4.3, West Sumatra is an elongated terrane wedged between the Woyla terrane to the southwest and the Sibumasu terrane to the northeast. This region of Southeast Asia is also often referred to as Sundaland. A more detailed tectonic map of these terranes is shown in Figure 4.4.

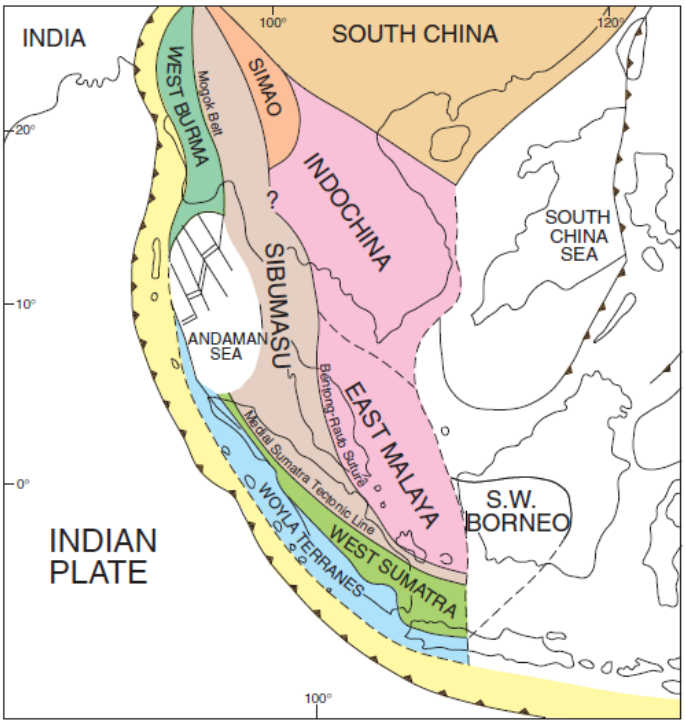

Figure 4.3: Continental tectonic blocks in Southeast Asia (Barber and Crow, 2009)

West Sumatra is composed mostly of Carboniferous aged units with a few Permian units, bounded to the northeast by Permo-Carboniferous units of Sibumasu (East Sumatra) and to the southwest by the younger Jurassic-Cretaceous units of the Woyla terrane (Figure 4.4). The contact between West Sumatra and the Sibumasu (East Sumatra) terrane is marked by the Medial Sumatra Tectonic Zone (MSTZ); this zone is marked by

highly deformed rocks including schists and gneisses, and is suggested to be the main locus of translation of West Sumatra outboard Sibumasu. Ultimately, understanding the tectonic events that placed West Sumatra outboard of Sibumasu may allow the Sumatra region to be used as an analogue to the Quebecia Arc.

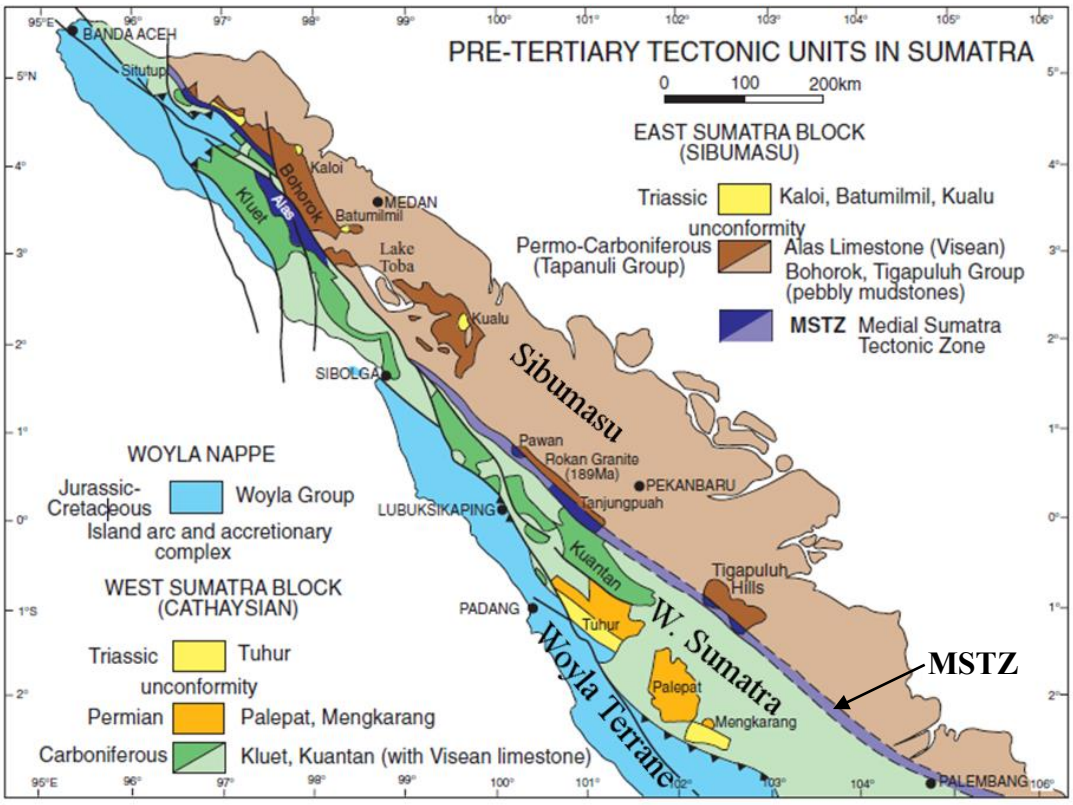

Figure 4.4: Distribution of the stratigraphic and tectonic units in Sumatra; darker shade indicate outcrop, lighter tons indicate areas where pre-Tertiary is overlain by Tertiary and Quaternary sediments (Barber and Crow, 2009)

In the Late Paleozoic, Asia as a whole was amalgamated from terranes derived from the northern margin of East Gondwana. Although Sibumasu and West Sumatra are of similar age, mapped floral and faunal data strongly suggests that these terranes had different origins (Barber and Crow, 2009); Sibumasu from western Gondwana, and West Sumatra from Cathaysia, a northern peripheral region of Gondwana (Figure 4.5). During

the Early Permian, Cathaysia was a peripheral region of Gondwana that would eventually make up the landmasses of China and South Asian countries, including the Sumatra region. In Figure 4.5, Cathaysia is shown as the collection of South China, East Malaya, Borneo and West Sumatra. Based on floral and faunal evidence, West Sumatra originated as a piece of Cathaysia, while Sibumasu came from western Gondwana.

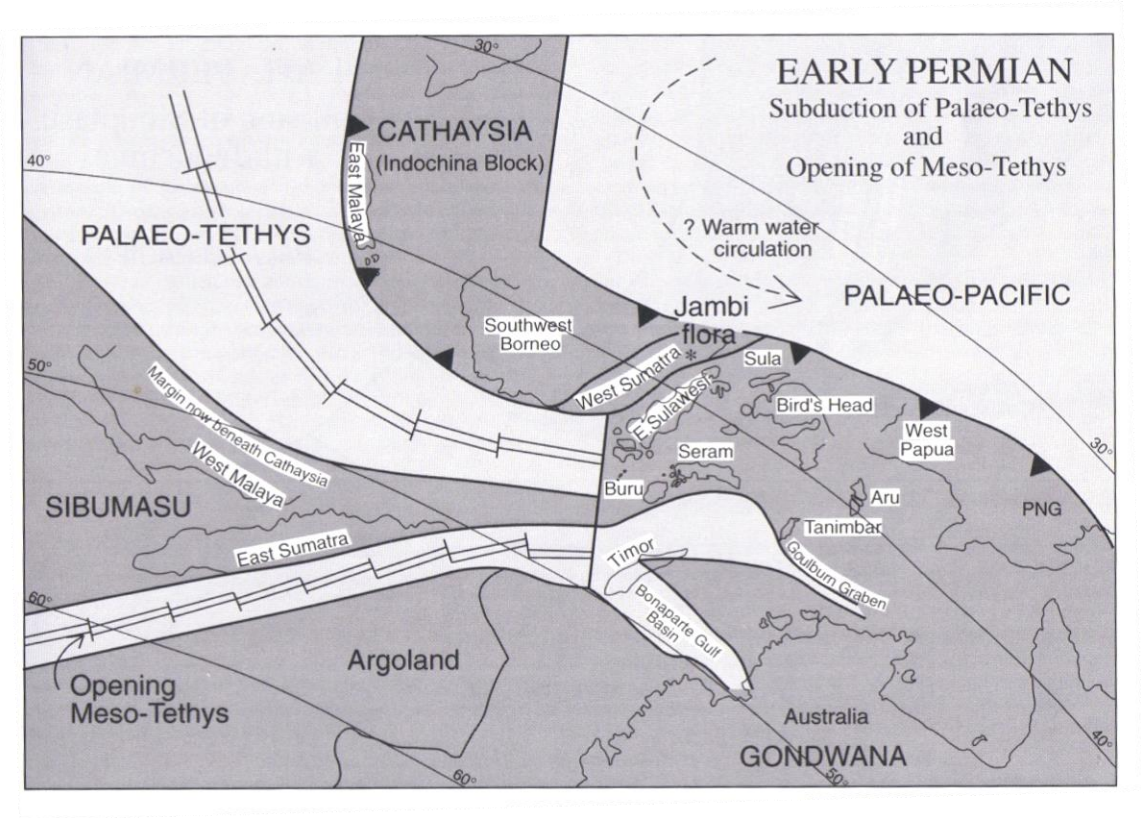

Figure 4.5: Paleogeography of NE Gondwana and SE Asian terranes in the Early Permian, showing the subduction of the Palaeo-Tethys between Sibumasu and Cathaysia, and the opening of the Meso-Tethys between Sibumasu and Gondwana (Barber et al., 2005).

The tectonic history of the Sumatra region can be loosely summarized in 3 major steps:

(1) While the Paleotethys was still spreading in the Early Permian, its northern margin began to subduct beneath Cathaysia. Meanwhile, Sibumasu began to rift from Western Gondwana (toward Cathaysia, Figure 4.5).

(2) In the late Permian to early Triassic, Sibumasu collided with Cathaysia (Figure 4.6).

(3) Strike-slip movement along the MSTZ placed West Sumatra outboard of Sibumasu (shown in Figure 4.7).

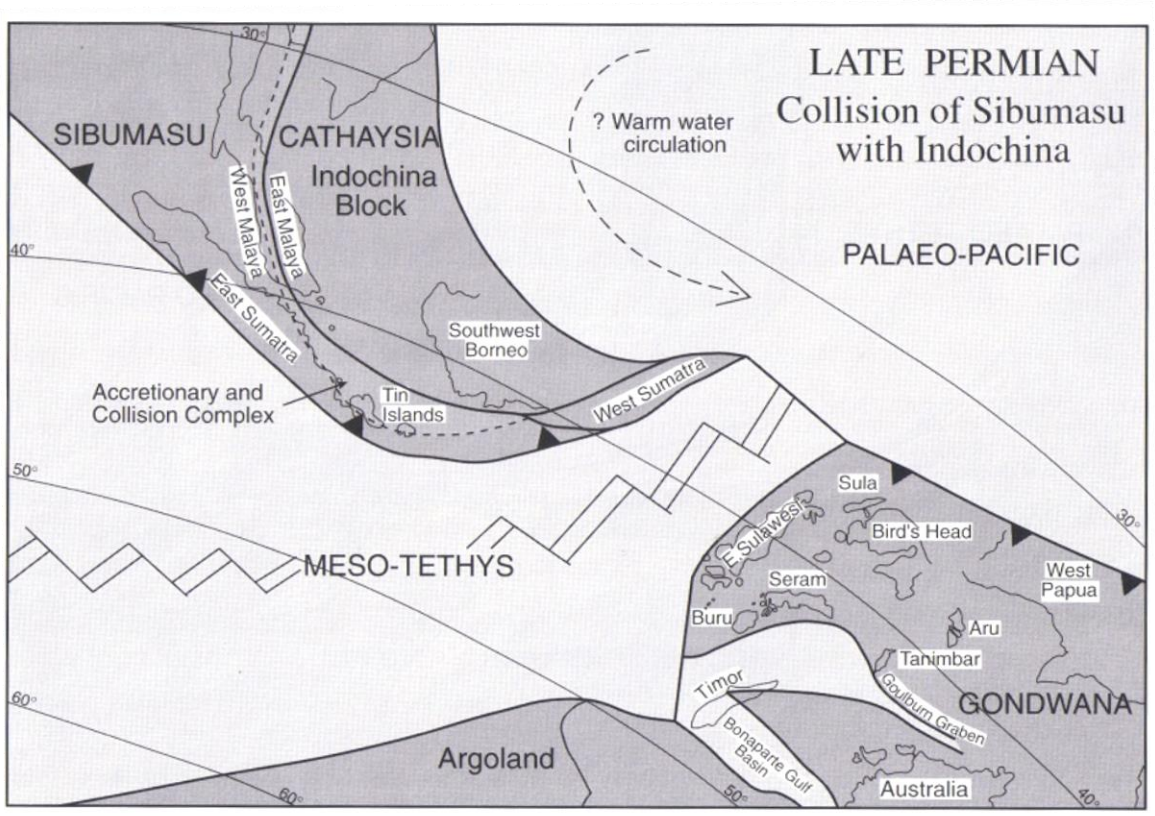

Figure 4.6: Paleogeography of NE Gondwana and SE Asian Terranes in the Late Permian (Barber et al., 2005)

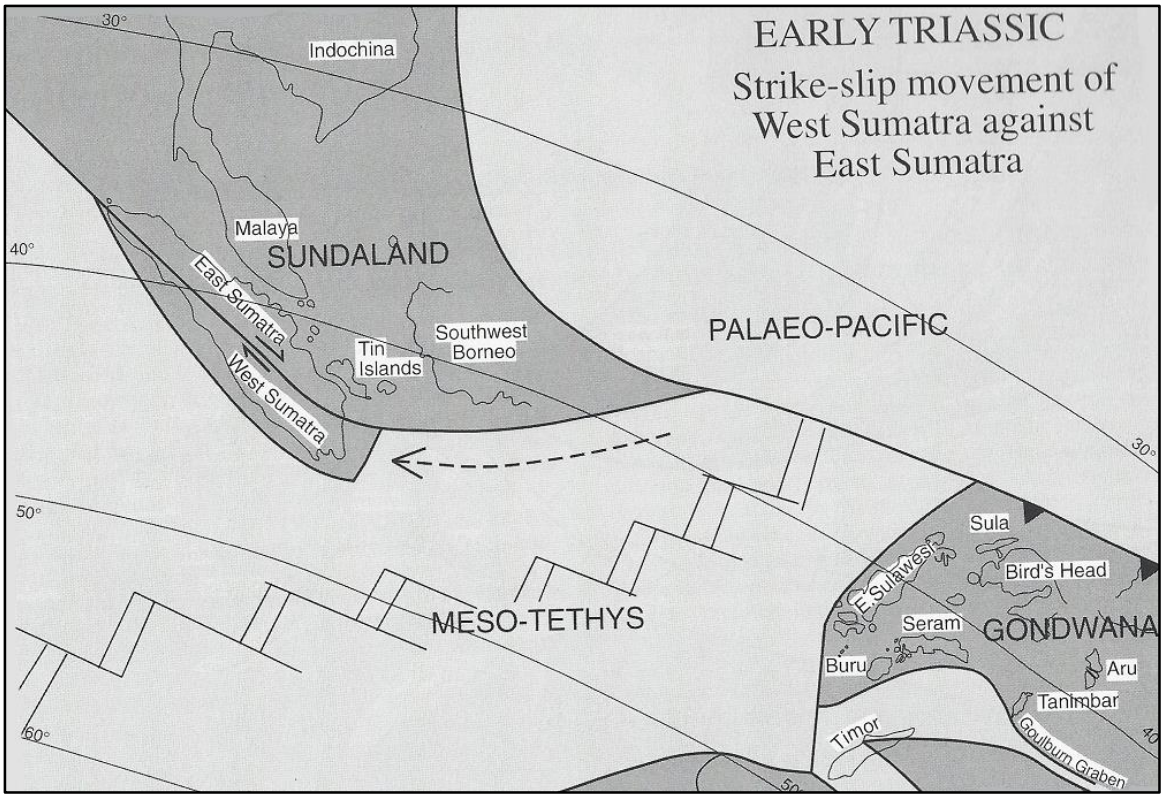

Figure 4.7: Paleogeographic map of the SE Asian terrane in the Early Triassic (Barber et al., 2005)

It is suggested that West Sumatra moved westwards from the southeastern extremity of Cathaysia (Figure 4.5) via strike-slip faulting along the MSTZ to its current position outboard of Sibumasu (shown in Figure 4.6 and 4.7 as East Sumatra). Hutchinson (1994) suggested that this translation occurred during the Cenozoic; However a comparison of Carboniferous, Permian and Triassic sequences of the eastern Sumatra Sibumasu Terrane shows continuity of Middle to Upper Triassic sediments across West Sumatra, the MSTZ, Sibumasu and Malaya (Figure 4.8) – suggesting that these blocks had their present relationships before Mid-Triassic times (Barber et al., 2005).

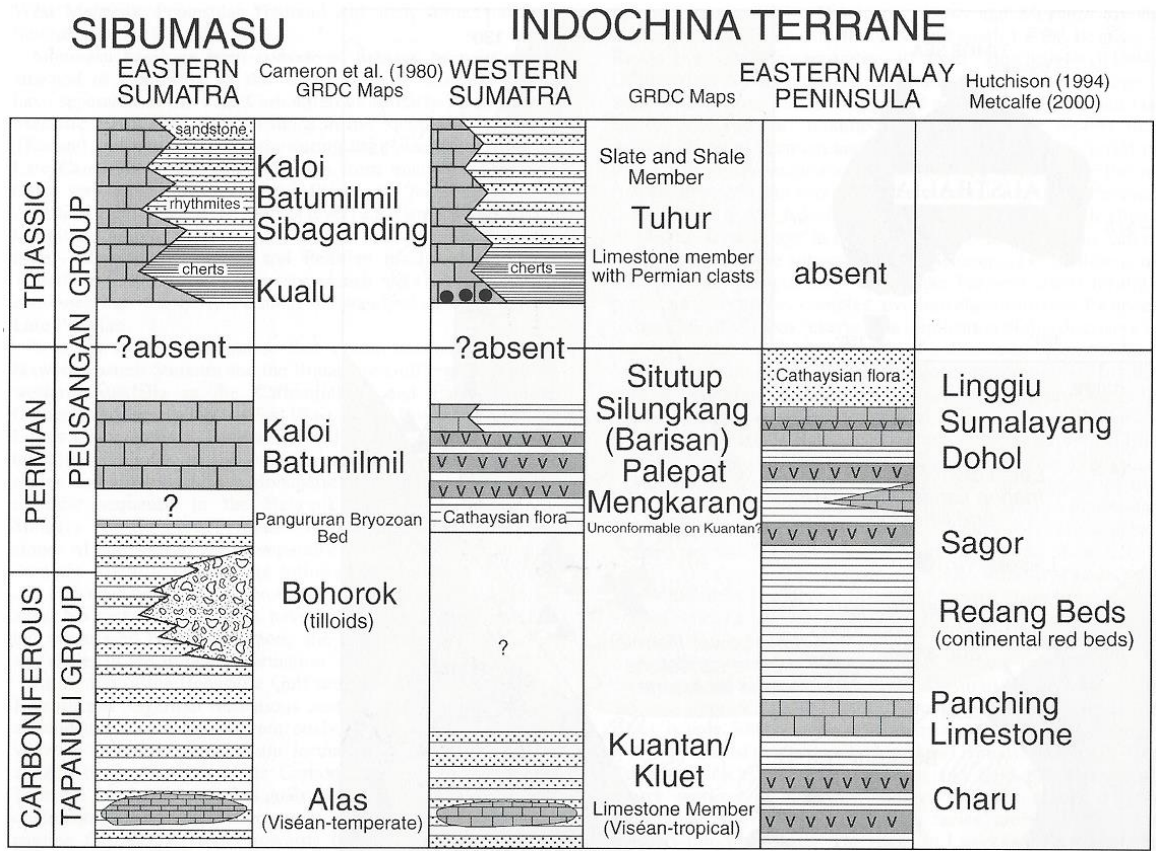

Figure 4.8: Comparisons of the sediment sequences in Sibumasu (Eastern Sumatra) and Western Sumatra (Barber and Crow, 2005)

These sedimentary sequences also show no record of sediments for the late Permian/early Triassic, therefore it is suggested that the translation of West Sumatra to its position outboard of Sibumasu occurred during this time (Barber et. al, 2005).

Therefore, using the detailed tectonic history of West Sumatra as an analogue, it is plausible that a Paleoproterozoic crustal panel was translated southwest from the Berthe Terrane during the accretion of Quebecia in multiple stages, causing it to become inserted between a north and south portion of the younger Mesoproterozoic Quebecia terranes.

4.3 Orogenic Model

Utilizing Barber and Crow's 2003 cross-section for the evolution of Sumatra as a basis, a similar model can be proposed for the tectonic history of the old crustal fragment within Quebecia (Figure 4.9). In this model, blocks are transported out of and into the line of cross section by transcurrent movement along the margin.

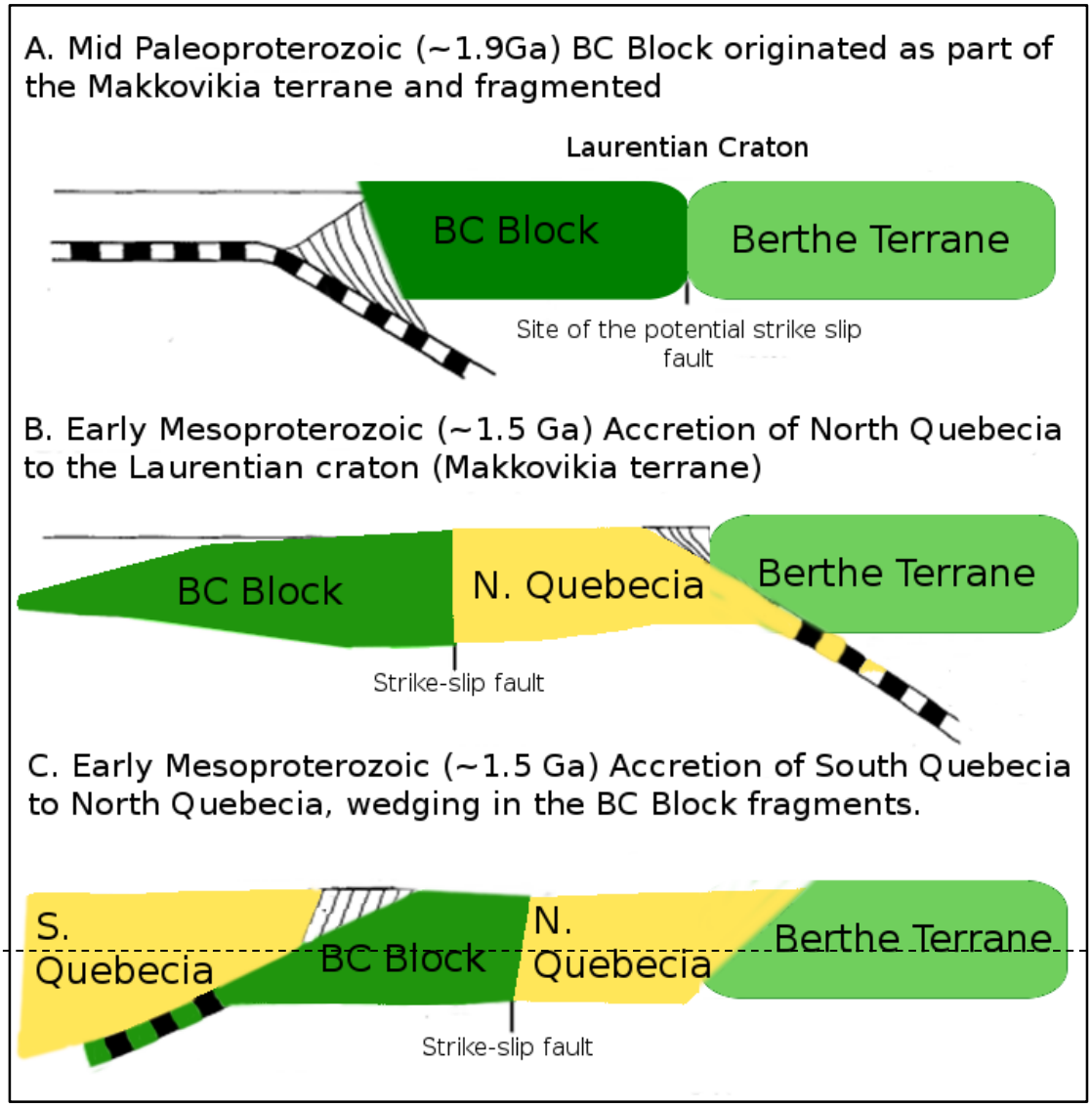

Figure 4.9: Proposed tectonic model for placement of the old block within the Quebecia Terrane (After Barber and Crow, 2003).

During the mid-Paleoproterozoic, the BC block was originally a piece of the Berthe Terrane to the north (Figure 4.9, A). Subduction under Laurentia began in the early Mesoproterozoic, bringing the Quebecia arc to accrete at the margin (Figure 4.9, B). Between these two periods, strike slip tectonics would have transported the BC block south from its origin similar to how the WSB was transported along the MSTZ to its current position outboard of Sibumasu. The BC block would have then reaccreted between a south and north portion of the Quebecia Terrane (Figure 4.9, C).

Chapter 5: Conclusions

The current study aimed to further outline the boundary of the Paleoproterozoic block defined by Dickin and Higgins (1992) and later Hynes (2010) in the Baie Comeau region of Central Quebec, Canada. Figure 5.1 shows a summary of the final mapped BC block fragments (dark green) and their spatial relation to their proposed origins in the Berthe Terrane (light green). The complete dataset allows a re-examination of the questions raised by Condie (2013) regarding gaps in the ages of crustal material on the Laurentian margin.

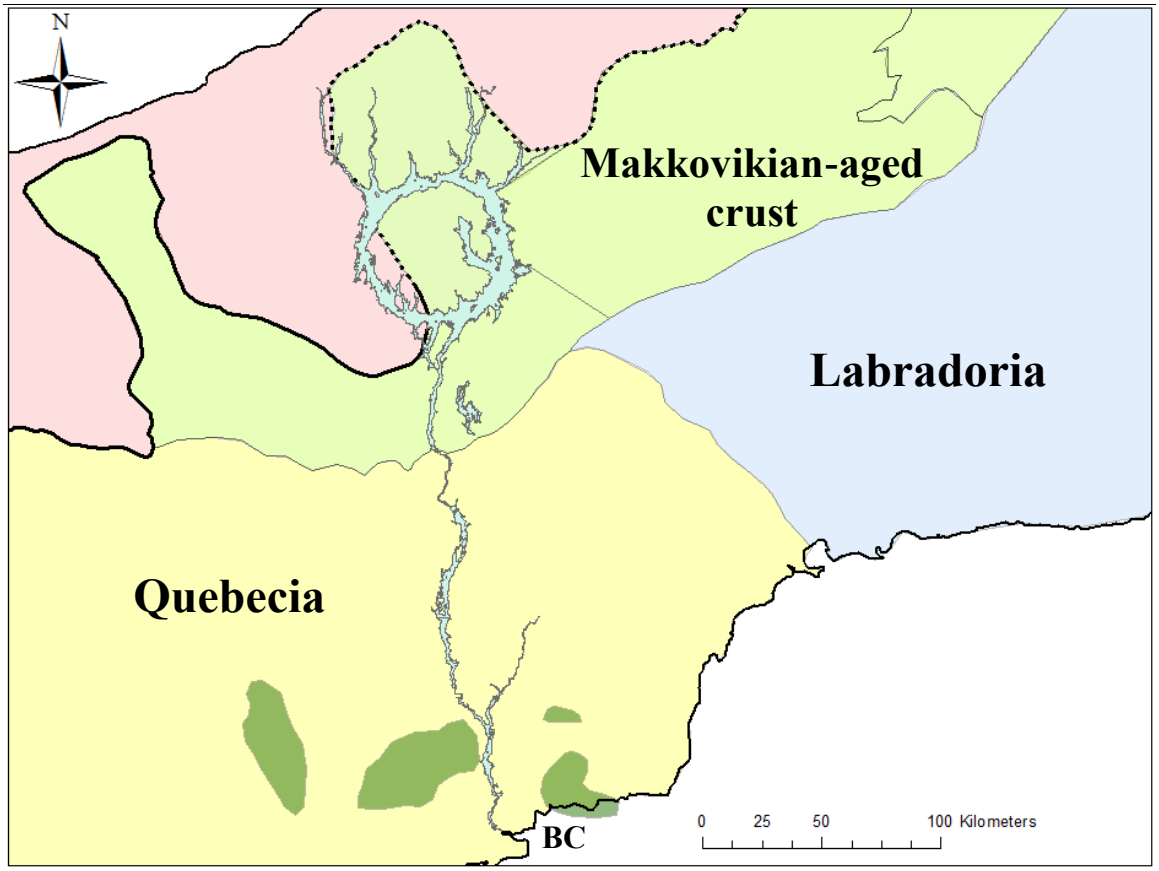

Figure 5.1: a map of the north eastern portion of the Grenville Province showing the old blocks (dark green), Quebecia (yellow), Makkovikian-age Berthe and Molson Lake Terranes (green), Labradoria (blue) and Archean (pink). BC: Baie Comeau.

Similar to Condie's zircon age histogram (Figure 1.5), Figure 5.2 presents a compilation of the data from the current study. The red bar (1.65-1.69 Ga) represents samples which are geographically located between areas of old and young crust, and therefore their intermediate ages are attributed to local mixing phenomena.

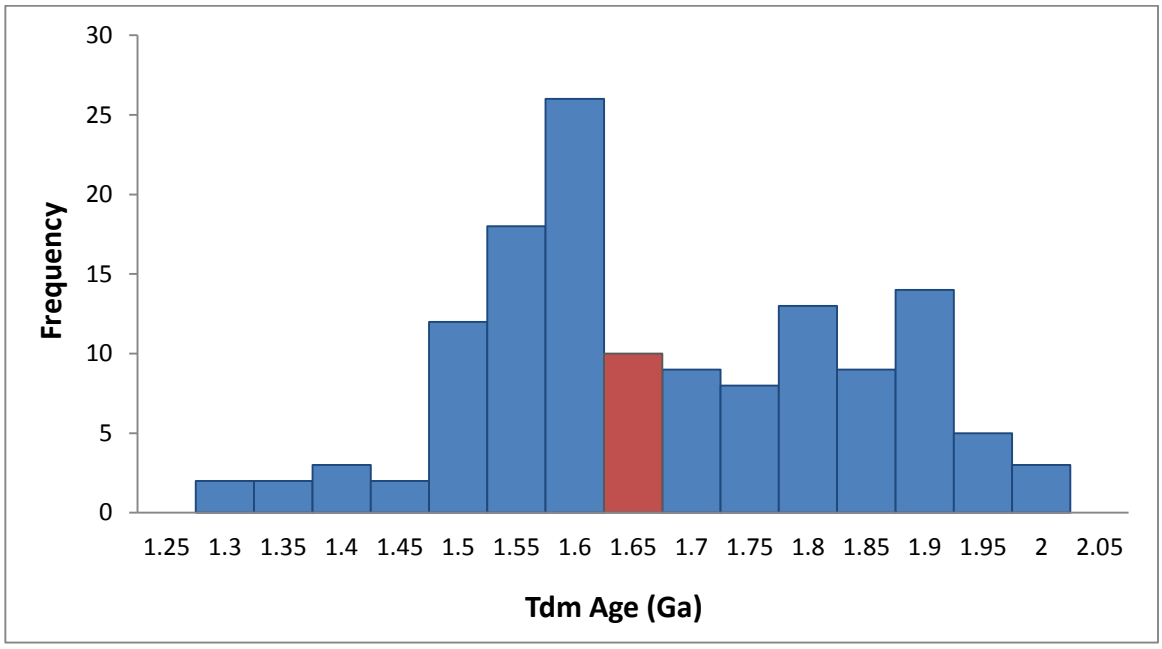

Figure 5.2: A histogram summary of the model ages for this study. Red bar indicates the border samples as outlined in Table B-3.

These locations are shown in Figure 5.3, which is an enlargement of the area around Baie Comeau to show the locations of the 1.65-1.69 Ga age samples relative to the older and younger crustal blocks. Based on their locations, these samples do not represent an actual crustal formation event and therefore indicate there is a real gap in crustal formation ages in the study area.

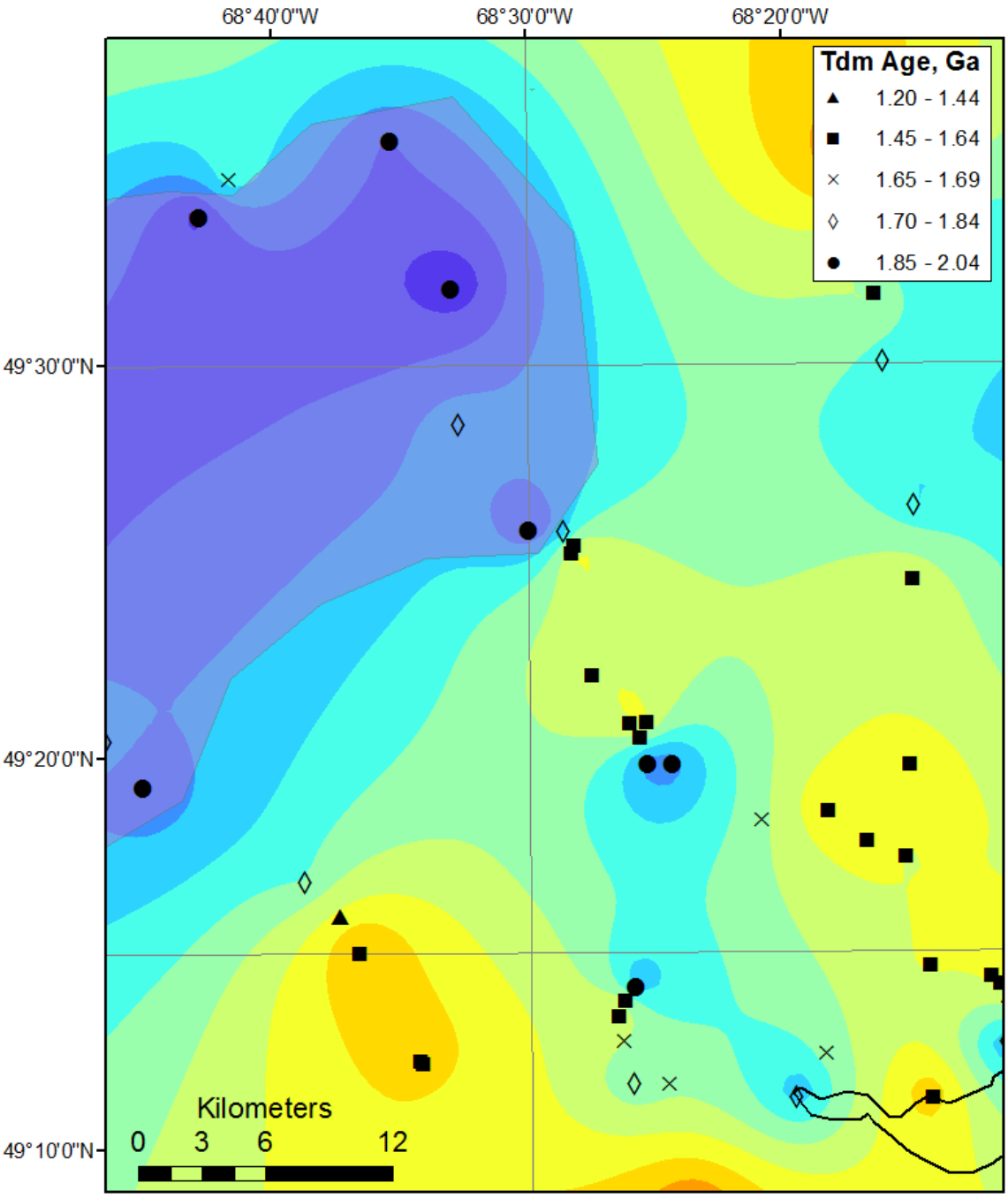

Figure 5.3: Enlargement of area around Baie Comeau, showing the boundary samples (X's) in relation to the surrounding blocks of old and young crust

The crustal formation age gap demonstrated in Figure 5.2 corresponds to Condie's gap in U-Pb zircon ages (Figure 1.5). This substantiates the case that there is a genuine gap in crustal formation between the Labradorian and Pinwarian events (the latter representing Quebecia).

Based on the modern analogue that was presented in Chapter 4, it is suggested that crustal evolution on the Laurentian margin during the Mesoproterozoic involved transport of crustal terranes along the continental margin during arc accretion processes. This suggests that the evolution of the margin did not involve major removal of crustal material, but simply rearrangement of existing terranes. Hence it is concluded that there is a genuine gap of crustal formation on the Laurentian margin between the Labradorian and Pinwarian events.

One of the issues raised by this argument is the question of the termination of the Labradorian terrane east of Manicouagan (Figure 5.1). It could be suggested that Labradorian-aged crust was removed by subduction, but Dickin (2000) argued that the original extent of Labradorian crust is marked by the extent of the Trans-Labrador Batholith (Figure 1.8). This late Labradorian igneous suite is associated with the accretion of the Labradorian terrane to Laurentia. The fact that it terminates just to the east of Manicouagan suggests that this was the original limit of the Labradorian terrane (Dickin, 2000).

In order to better understand the possible point of origin of the old crustal panels in the Baie Comeau area, it would be necessary to conduct more detailed mapping of the western continuation of the Berthe Terrane (Figure 5.1). This is an area with poor access

that has not been mapped in detail, but additional study of the boundary between Makkovikian/Labradorian and Pinwarian aged crust could clarify whether this is a suitable site for the detachment of the Baie Comeau old crustal fragments.

Since Quebecia is now divided into north and south terranes to accommodate an old panel, it should now be regarded as a Composite Arc Belt. A similar idea was proposed in Ontario for a Composite Arc Belt within the Central Metasedimentary Belt (Carr et al., 2000), but Dickin and McNutt (2007) argued that the proposed Composite Arc Belt of Ontario is actually a failed back arc rift zone. This conclusion was based on the geometry of the model age distribution, the presence of alkaline rocks and marbles, and the rift-like geochemistry of mafic volcanics and intrusions (Smith and Holm, 1990). In the present study none of the above criteria are met, and the Quebecia Composite Arc Belt consists of much larger accreted terranes with distinct ages and calc-alkaline signatures, making it a much more convincing candidate for a Composite Arc Belt.

References

Bachelor, R.A., and Bowden, P. (1985). Petrogenetic interpretation of granitoid rock series using multicationic parameters. *Chemical Geology*, **48**, 43-55.

Barber, A.J. and Crow, M.J. (2003). Evaluation of Plate Tectonic models for the development of Sumatra. *Gondwana Research*, **20**, 1-28.

Barber, A. J., Crow, M. J. and Milsom, J. S. (2005). Sumatra: Geology, Resources and Tectonic Evolution. *Geological Society Memoir no. 31*.

Barber, A.J. and Crow, M.J. (2009). The structure of Sumatra and its implications for the tectonic assembly of Southeast Asia and the destruction of Paleothethys. *Island Arc*, **18**, 3-20.

Carr, S.D., Easton, R.M., Jamieson, R.A., Culshaw, N.G. (2000). Geologic transect across the Grenville orogeny of Ontario and New York. *Can. J. Earth Sci*. **37**, 193-216.

Condie, K.C. (2002). Breakup of a Paleoproterozoic supercontinent. *Gondwana Res*., **5**, 41-43.

Condie, K.C. (2013). Preservation and recycling of crust during accretionary and collisional phases of Proterozoic orogens: A bumpy road from Nuna to Rodinia. *Geosciences*, **3**, 240-261.

Debon, F., and LeFort, P. (1983). A chemical-mineralogical classification of common plutonic rocks and associations. Trans. R. Soc. Edinb. *Earth Sci.,* **73**, 135–149.

DePaolo, D.J. (1981). Neodymium isotopes in the Colorado Front Range and crust – mantle evolution in the Proterozoic. *Nature,* **291**, 193-7.

DePaolo, D.J. and Wasserburg, G.J. (1976a). Nd isotopic variations and petrogenic models. *Geophys. Res. Lett,*. **3**, 249-252.

DePaolo, D.J. and Wasserburg, G.J. (1976b). Inferences about magma sources and mantle structure from variations in $^{143}Nd/^{144}Nd$. *Geophys. Res. Lett.,* **3,** 743-746.

Dickin, A.P., and Higgins, M. (1992). Sm/Nd evidence for a major 1.5 Ga crust-forming event in the central Grenville province. *Geology*, **20**, 137–140.

Dickin, A.P., and McNutt, R.H. (2007). The Central Metasedimentary Belt (Grenville Province) as a failed back-arc rift zone: Nd isotope evidence. *Earth and Planetary Science Letters*, **259**, 97-106.

Dickin, A.P. (2000). Crustal formation in the Grenville Province: Nd isotope evidence. *Canadian Journal of Earth Sciences*, **37**, 165-181.

Dickin, A.P. (2005). Radiogenic Isotope Geology 2nd Edition. Cambridge: Press Syndicate of the University of Cambridge.

Green, T.H., Brunfeldt, A.O., and Heier, K.S. (1969). Rare earth element distribution in anorthosites and associated high grade metamorphic rocks, Lofoten-Vesteraalen, Norway. *Earth and Planetary Science Letters,* **7**, 93-8.

Hutchinson, C.S. (1994). Gondwana and Cathaysian blocks, Palaeothethys sutures and Cenozoic tectonics in South-East Asia. *Geologische Rundshau*, **82**, 388-405.

Hynes, A., Indares, A., Rivers, T., and Gobeil, A. (2000). Lithoprobe line 55: integration of out of phase seismic results with surface structure, metamorphism and geochronology, and the tectonic evolution of the eastern Grenville Province. *Canadian Journal of Earth Sciences,* **37**, 341–358.

Hynes, E. (2010). Nd isotope delineation of crustal terranes in the Bancroft area of Ontario and the Saguenay and Baie Comeau regions of Central Quebec: Ensialic rifting and arc formation. *MSc Thesis, McMaster University*.

Jagoutz, O.E., Burg, J.P., Hussain, S., Dawood, H., Pettke, T., Iizuka, T., and Maruyama, S. (2009). Construction of the granitoid crust of an island arc part I: geochronological and geochemical constraints from the plutonic Kohistan (NW Pakistan). *Contrib Mineral Petrol,* **158**, 739-755.

Kerr, A. and Fryer, B.J. (1994). The importance of late and post orogenic crustal growth in the Early Proterozoic: Evidence from Sm-Nd isotopic studies of igneous rocks in the Makkovik Province, Canada. *Earth and Planetary Science Letters,* **125**, 71-88.

Ketchum, J.W.F., Culshaw, N.G., and Barr, S.M. (2002). Anatomy and orogenic history of a Paleoproterozoic accretionary belt: the Makkovik Province, Labrador, Canada. *Canadian Journal of Earth Sciences,* **39**, 711-730.

Kimmerle, S. (2014). Nd Isotope mapping near Manicouagan, Grenville Province of Quebec. *BSc Thesis, McMaster University.*

Le Bas, M.J., Lemaitre, R.W., Streckeisen, A. and Zanettin, B. (1986). A Chemical Classification of Volcanic-Rocks Based on the Total Alkali Silica Diagram. *Journal of Petrology, 27*, 745-750.

McCulloch, M.T, and Wasserburg, G.J. (1978). Sm-Nd and Rb-Sr chronology of continental crust formation. *Science*, **200**, 1003-11.

McMenamin, M.A.S., and McMenamin, D.L.S. (1990). The emergence of animals: The Cambrian breakthrough: New York, Columbia University Press.

Moumblow, R. (2014). Nd isotope mapping of crustal boundaries within the Eastern Grenville and Makkovik Provinces, Southern Labrador. *PhD Thesis, McMaster University.*

Nelson, B. K. and DePaolo, D.J. (1984). 1700 Myr greenstone volcanic successions in southwestern North America and isotopic evolution of Proterozoic mantle. *Nature*, **312**, 143-6.

Pesonen, L.J., Mertanen, S., and Veikkolainen, T. (2012). Paleo-Mesoproterozoic supercontinents—a paleomagnetic view. *Geophysica,* **48**, 5–48.

Piper, J.D. (1987). Palaeomagnetism and the Continental Crust. New York: Wiley.

Rivers, T., Martignole, J., Gower, C.F., and Davidson, A. (1989). New tectonic divisions of the Grenville Province, southeastern Canadian Shield. *Tectonics* **8**, 63–84.

Rivers, T. (1997). Lithotectonic elements of the Grenville Province: review and tectonic implications. *Precambrian Research*, **86**, 117-154.

Rogers, J.J.W. and M. Santosh. (2002). Configuration of Columbia, a Mesoproterozoic supercontinent, *Gondwana Res.,* **5**, 5–22

Sawkins, F.J. (1976). Widespread continental rifting: some considerations of timing and mechanism. *Geology*, **4**, 427-430.

Slaman, L. (2013). Nd Model Age Mapping and Crustal Evolution of the Manicouagan Region, Quebec. *BSc Thesis, McMaster University*.

Smith, T.E., Holm, P.E. (1990). The geochemistry and tectonic significance if pre-metamorphic minor intrusions of the Central Metasedimentary Belt, Grenville Province, Canada. *Precambrian Research*, **48**, 341-360.

Spray, J.G., Thompson, L.M., Biren, M.B., and O'Connell-Cooper, C. (2010). The Manicouagan impact structure as a terrestrial analogue site for lunar and martian planetary science. Planet. *Space Sci.,* **58**, 538–551.

Système d'information géominière du Québec. *Energie et Ressources naturelles, Québec*.Gouvernement du Québec. Accessed September, 2014. <http://sigeom.mrn.gouv.qc.ca/signet/classes/I1108_afchCarteIntr?l=a>

Thomson, S.D., Dickin, A.P., and Spray, J.G. (2011). Nd isotope mapping of Grenvillian crustal terranes in the vicinity of the Manicouagan Impact Structure. *Precambrian Research*, **191**, 184-193.

Wegner, A. (1967). The Origin of Continents and Oceans. English translation of 4th edition [1929]. London: Methuen.

Wilson, J. T. (1966). Did the Atlantic close and then re-open? *Nature*, **211**, 676–681.

Wynne-Edwards, H.R., (1972). The Grenville Province. *Geological Association of Canada Special Paper,* **11**, 263-334.

Zelek, M. and Dickin, A. (2013). Nd isotope mapping of crustal terranes in the Parent-Clova area, Quebec: Implications for the evolution of the Laurentian margin in the Central Grenville Province. *Geosciences*, **3**, 448-465.

Appendix A: Field and Laboratory Techniques

A1 – Introduction

The analysis for the Sm-Nd method involves three broad steps of field collection and sample powdering, chemical processes on the samples, and mass spectrometry. Each step has an associated well-defined methodology as described below, and must be followed precisely in order to ensure repeatability and valid, comparable results.

A2 Field Sample Collection

Orthogneiss samples were collected at road cut outcrops within Central Quebec. Sample distribution was primarily controlled by presence and access of logging roads and availability of outcrop within the study areas. Sample selection was based on the availability of fresh, unweathered and relatively homogenous rocks, so that the crustal formation of that rock sample would be accurate representation of the unit as a whole. A 12 lb. sledge hammer and crow bar was used to extract the samples, as well as utilization of proper personal safety equipment. At each location a GPS reading was taken and sample location was recorded on the site map.

A3 Pulverization

To prepare samples for chemical dissolution, they first have to be crushed into a fine powder within the rock crush room on McMaster University campus. First, samples were scrubbed with a wire brush in order to remove any contamination such as moss and dirt, and then using a hydraulic splitter, the samples were split into smaller ~5cm^3 pieces.

These pieces were then processed through a jaw crusher, which first would be contaminated with some of the current sample in order to avoid dust contamination from previous samples. The jaw crusher would grind the sample into gravel sized ~1cm^3 pieces. The gravel would then be divided in half using a table top random sorter, leaving behind enough to fill and run a disc mill, yielding a powdered sample.

A4 Chemical Dissolution

Teflon coated plastic bombs were labelled with the sample name and treated to remove static to avoid mass inaccuracies. Each bomb, with lid, was then placed on an analytical scale and their weight recorded. 150mg of sample powder was added to each corresponding bomb with a clean spatula, reweighed and recorded.

In order to separate the Neodymium and Samarium from the sample, silicate and carbonate components must first be dissolved. This dissolution of the sample powder took place in the Spectrochemistry Clean Lab at McMaster University. The bombs were lined up in a fume hood where 10ml of Hydrofluoric Acid (HF) was added to each and the lids secured tightly. The bombs were then placed in protective plastic jackets and placed in a 140°C oven for 4 days. The bombs were then removed when cooled, and then placed on hot plates for evaporation. After the HF was evaporated, 5ml of concentrated nitric acid (HNO_3) was loaded in each and the bombs were returned to the hotplates. After evaporation, 5ml of 6 molar Hydrochloric Acid (HCl) was added to each bomb and again placed in the oven overnight. WHIMIS protocol for handling hazardous chemicals was followed at all times.

The samples were then split so that both isotope ratio (IR) and isotope dilution (ID) analysis can be performed. Samples are first diluted with 10ml of de-ionized water and then bomb, sample, and lid, were placed on the analytical scale to be weighed and recorded. Each sample was then split into two beakers, one for IR and one for ID, where samples marked ID were then spiked with a ^{150}Nd-^{149}Sm enriched solution. This process was done by weighing the spike bottle, tarring the mass and adding approximately 150mg of spike to each sample. The spike bottle would then be reweighed and the amount of spike recorded. After completion, beakers were then placed on hotplates for evaporation.

A5 Chromatography

In order to concentrate the Neodymium and Samarium in each sample, column chemistry was conducted in two stages. The first stage uses the method of cation exchange chromatography, which separates major elements and isolates the rare earth elements (REE) based on their binding affinities to the resin within the columns. The second stage is Rare Earth Element Chromatography, which separates out Nd and Sm.

In preparation for the first stage cation columns, 0.4 M HCl was used to dissolve the samples to a total of 2ml within test tubes and then centrifuged. 1ml of each sample was loaded with a pipette into the cation columns, and then washed through with 20ml of 3 M HNO_3, which removes Na, Ca and other major elements. 10ml of 3 M HNO_3 is then washed through to collect the REEs. After collection, the

samples were placed under heat lamps for evaporation and 1mL of 0.4 M HCl was added in order to load the samples into the next stage of columns.

Next 1ml of each sample was loaded using a pipette into the REE chromatography columns. The samples were washed through with 10ml of 0.4 M HCl, then 10ml of 0.4 M HCl to collect the Nd in all samples. Next, for just the ID samples, 2ml of 1 M HCl was washed through, and then 12ml of 1 M HCl was used to collect the Sm. The resulting samples were evaporated under heat lamps. One drop of 0.0003 M H_3PO_4 was added to the residue once dry, and then evaporated again until near dryness.

A6 Isotopic Analysis via Mass Spectrometry

The samples were then prepared to be loaded into the VG isomass 345 mass spectrometer in the Isotope Geochronology lab at McMaster University. 0.4µL of 0.2 molar H_3PO_4 was added to the dried samples and the solution was then loaded on the center of a double rhenium tantalum filament bead. A 2 amps current was then passed through the bead to dry the sample, and then the beads were loaded into the mass spectrometer for analysis.

A La Jolla standard was run with every barrel and produced a mean value of0.511855. The resulting analyses for the duration of this study are shown in Table A-1. All spiked samples analyses with a run precision >0.02% were rejected or repeated, along with unspiked samples with a run precision of >0.01%.

Appendix B: Data Tables

Table B-1: Nd isotope analysis results for Quebecia samples (1.46-1.64 Ga) in the study area.

Map #	Sample	Easting	Northing	Nd ppm	Sm ppm	Sm147	Nd143	WRP	Tdm (G)
Quebecia (<1.65Ga)						Nd144	Nd144		
1	PI11	411169	5474428	52.0	11.56	0.1345	0.512263	0.011	1.50
2	PI10	415227	5470693	40.1	8.25	0.1243	0.512118	0.013	1.57
3	PI32	426340	5440750	40.6	8.83	0.1315	0.512209	0.011	1.54
4	PI 1	437315	5455428	36.1	6.80	0.1139	0.512052	0.011	1.51
5	PI33	448510	5460560	74.5	14.40	0.1167	0.512123	0.022	1.44
	PI33R			75.1	14.86	0.1196	0.512170	0.011	1.41
6	PI23	453032	5426200	127.3	22.28	0.1059	0.512004	0.013	1.47
	PI23 R			75.5	13.12	0.1050	0.511995	0.009	1.47
7	PI25	445278	5436567	10.8	1.79	0.1005	0.511903	0.015	1.53
8	PI24	446868	5430992	46.3	9.09	0.1185	0.512104	0.014	1.50
9	PI22	458205	5422647	28.6	4.64	0.0979	0.511901	0.011	1.50
10	PI21	471499	5414452	27.1	4.73	0.1055	0.511944	0.012	1.55
11	PI20	474053	5409209	38.7	6.60	0.1030	0.511980	0.014	1.46
12	FV24	449018	5514007	80.1	16.45	0.1242	0.512076	0.010	1.64
13	FV20	439660	5499750	25.2	5.76	0.1383	0.512269	0.010	1.56
14	FV19	440430	5496410	48.4	10.57	0.1319	0.512170	0.012	1.62
15	FV41	464567	5452464	74.3	13.24	0.1078	0.511919	0.014	1.61
16	FV9	467360	5449220	45.0	8.39	0.1126	0.512094	0.012	1.43
17	FV6	472460	5445900	24.0	4.33	0.1089	0.511951	0.009	1.59
18	FV32	480756	5432720	72.7	11.00	0.0914	0.511874	0.014	1.46
19	FV31	493168	5414655	45.8	7.40	0.0977	0.511883	0.008	1.52
20	n20**	498400	5406200	12.3	2.31	0.1143	0.512014	0.012	1.57
21	BC66	491720	5502230	85.7	15.34	0.1082	0.512027	0.012	1.47
22	BC62	500260	5495860	27.6	5.92	0.1298	0.512204	0.016	1.52
23	BC58	527390	5457040	35.6	8.42	0.1450	0.512470	0.023	1.27
	BC58R			25.2	5.99	0.1437	0.512471	0.017	1.24
24	BC30	528276	5455362	153.5	25.90	0.1020	0.511973	0.013	1.46
25	BC18*	531190	5450230	105.63	14.51	0.0830	0.511758	0.025	1.50
26	BC17*	531310	5450150	52.55	11.03	0.126929	0.512156	0.024	1.55
27	BC19*	532420	5438440	46.72	9.91	0.128283	0.512169	0.013	1.56
28	m132**	518000	5546400	39.52	8.60	0.1315	0.512197	0.012	1.56
29	m121**	517700	5536400	16.07	3.01	0.1131	0.512016	0.012	1.55
30	ma114**	518300	5530400	20.36	2.78	0.0835	0.511855	0.012	1.39
31	m103**	517900	5520500	45.43	9.32	0.1241	0.512116	0.012	1.57
32	SV53	533610	5524100	50.3	11.08	0.1332	0.512230	0.013	1.52
33	SV52	533720	5518590	103.4	19.13	0.1119	0.512025	0.010	1.52
34	SV50	532990	5513000	98.6	16.90	0.1036	0.511973	0.013	1.48
35	BC54	538426	5474664	21.9	4.26	0.1176	0.512050	0.010	1.57
36	ma40**	538300	5474300	27.18	5.46	0.1214	0.512097	0.012	1.56

Table B-1 Continued

Map #	Sample	Easting	Northing	Nd ppm	Sm ppm	Sm147	Nd143	WRP	Tdm (G)
Quebecia (<1.65Ga)						Nd144	Nd144		
37	BC5*	539290	5468490	18.20	4.05	0.1334	0.512202	0.024	1.59
38	MX5	541027	5466237	15.1	3.20	0.1282	0.512148	0.014	1.59
39	BC53	541832	5466329	40.8	7.78	0.1153	0.512034	0.016	1.56
40	MX6	541546	5465554	18.2	3.77	0.1253	0.512090	0.014	1.63
41	MX31	540888	5453128	34.7	7.15	0.1244	0.512107	0.010	1.59
42	MX32	540547	5452397	23.9	4.90	0.1239	0.512099	0.013	1.60
43	MX12	544294	5443177	79.0	14.86	0.1137	0.512139	0.010	1.37
	MX12R			59.8	11.24	0.1136	0.512146	0.014	1.36
44	BC16*	544290	5443160	85.06	16.03	0.1139	0.512121	0.019	1.40
45	SV47	558410	5526420	30.7	6.26	0.1232	0.512137	0.016	1.52
46	SV48	564890	5527470	33.7	6.55	0.1176	0.512103	0.012	1.49
47	SV43	555290	5514170	32.6	6.50	0.1204	0.512120	0.011	1.51
48	MX24	551934	5492440	55.7	7.55	0.0820	0.511879	0.010	1.35
49	MX22	552560	5486628	21.0	5.15	0.1485	0.512340	0.010	1.63
	MX22R			24.2	5.98	0.1495	0.512389	0.009	1.55
50	MX18	554398	5473099	15.2	2.42	0.0965	0.511829	0.015	1.58
51	bc9*	554300	5464340	29.2	5.71	0.1184	0.512054	0.012	1.58
52	BC7*	550410	5462130	26.00	5.47	0.1271	0.512169	0.015	1.54
53	ma12**	552300	5460700	4.38	0.85	0.1167	0.512045	0.012	1.57
54	BC8*	554100	5459970	18.83	4.53	0.1455	0.512322	0.021	1.61
55	BC10*	555260	5454820	22.66	5.19	0.1384	0.512258	0.022	1.59
56	MX9	555417	5448557	17.9	4.14	0.1402	0.512320	0.012	1.48
57	SV9	563059	5464881	11.2	1.74	0.0935	0.511746	0.015	1.64
58	SV10	562003	5460996	107.0	17.49	0.0988	0.511895	0.014	1.52
59	SV15	561170	5455440	29.1	6.88	0.1429	0.512413	0.012	1.35
60	sv14	561920	5455350	21.6	5.05	0.1416	0.5123231	0.014	1.52
61	BC51	558187	5454333	30.8	5.29	0.1037	0.511897	0.017	1.59
62	MX26	558561	5453955	33.4	6.16	0.1115	0.511978	0.013	1.58
63	BC50	558991	5453339	18.0	3.47	0.1169	0.512226	0.013	1.29
64	SV38	573400	5492640	22.0	3.29	0.0902	0.511728	0.016	1.62
65	SV21	598540	5478770	26.7	4.80	0.1087	0.511976	0.011	1.55
66	sv26	600200	5470740	25.2	5.36	0.1287	0.512166	0.015	1.57
67	n29**	599600	5466600	13.43	2.60	0.1171	0.512081	0.012	1.51
68	sv20	597630	5465510	29.0	5.26	0.1096	0.511993	0.013	1.54
69	n31**	605400	5473400	n/a	n/a	0.1208	0.512091	0.012	1.56
70	SV25	617230	5474060	37.6	7.82	0.1256	0.512123	0.011	1.59
71	n32a**	617800	5463800	42.79	7.78	0.1099	0.511981	0.012	1.56
72	n32b**	617800	5463800	32.07	6.29	0.1186	0.512059	0.012	1.57
73	SV24	628100	5483100	34.7	7.56	0.1319	0.512219	0.010	1.53

Table B-2: Nd isotope analysis results for BC Block samples (1.7-2.0 Ga) in the study area.

Map #	Sample	Easting	Northing	Nd ppm	Sm ppm	Sm147	Nd143	WRP	Tdm (G)
BC Block (1.7-2.0 Ga)						Nd144	Nd144		
74	FV23	448038	5508638	24.4	5.61	0.1387	0.512058	0.012	2.00
75	FV21	448602	5500027	43.6	10.07	0.1395	0.512138	0.009	1.86
76	FV18	441170	5495630	31.4	5.65	0.1087	0.511872	0.008	1.70
77	FV17	441580	5494580	37.3	6.50	0.1053	0.511713	0.012	1.87
78	FV16	444970	5491210	54.5	11.60	0.1288	0.512049	0.012	1.78
79	FV15	446980	5487460	44.9	9.28	0.1248	0.512013	0.011	1.76
80	FV14	449600	5484110	47.5	10.93	0.1390	0.512159	0.009	1.80
81	FV13	451030	5481450	41.0	8.05	0.1187	0.511888	0.020	1.85
82	FV11	457490	5468000	43.8	8.58	0.1184	0.511843	0.012	1.92
83	FV10	461860	5458480	35.3	7.06	0.1210	0.511912	0.010	1.86
84	PI28	443689	5451490	24.3	5.45	0.1352	0.512121	0.013	1.79
85	PI27	441966	5443150	40.4	7.41	0.1110	0.511816	0.013	1.82
86	FV34	467118	5450520	34.9	6.08	0.1052	0.511758	0.012	1.80
87	FV7	469620	5447800	33.6	6.58	0.1184	0.511973	0.015	1.71
88	FV5	480370	5435610	26.7	5.80	0.1317	0.512108	0.011	1.73
89	FV3	485460	5424460	40.0	8.90	0.1343	0.512116	0.009	1.78
90	FV43	490510	5419885	45.0	9.91	0.1330	0.512130	0.013	1.72
91	BC45	502240	5484700	49.5	9.79	0.1196	0.511879	0.010	1.88
92	BC43	503090	5477350	56.2	10.81	0.1163	0.511811	0.009	1.93
93	BC41	507740	5474930	46.1	8.93	0.1170	0.511874	0.011	1.84
94	BC38	512800	5472500	51.0	9.79	0.1160	0.511834	0.010	1.88
95	BC37	512940	5470020	53.1	10.37	0.1181	0.511897	0.010	1.82
96	BC36	513300	5469120	49.2	9.20	0.1130	0.511856	0.013	1.79
97	BC35	515000	5466270	73.6	15.62	0.1284	0.512045	0.012	1.78
98	BC34	516280	5465350	30.5	5.87	0.1163	0.511909	0.015	1.77
99	BC32	518060	5463110	54.7	10.70	0.1183	0.511878	0.010	1.86
	BC32r			51.4	10.13	0.1191		0.016	
100	BC31	525753	5458688	26.9	5.81	0.1305	0.512103	0.013	1.72
101	MA67**	529700	5493700	42.21	8.56	0.1226	0.511925	0.012	1.87
102	BC1*	520710	5490080	50.32	10.08	0.1210	0.511852	0.024	1.96
103	MA58.1**	532600	5486700	49.16	9.50	0.1168	0.511791	0.012	1.97
104	BC4*	532930	5480320	22.29	4.97	0.1348	0.512135	0.012	1.750
105	MA42.7**	536300	5475300	14.94	3.11	0.1257	0.511960	0.012	1.87
106	MX1	537956	5475316	44.4	8.11	0.1103	0.511808	0.012	1.82
107	BC52	541897	5464262	58.2	11.62	0.1207	0.511905	0.015	1.86
108	MA25.8**	543100	5464300	26.90	5.40	0.1212	0.511911	0.012	1.86
109	MX16	541385	5453756	29.0	5.59	0.1164	0.511846	0.013	1.87
110	MX14	541280	5449224	12.8	2.51	0.1184	0.511966	0.012	1.72
	MX14R			11.7	2.30	0.1190	0.511990	0.030	1.69
111	BC15*	548980	5448590	9.64	2.09	0.1312	0.512051	0.016	1.83
112	MX23	554025	5489780	28.4	6.20	0.1319	0.512047	0.017	1.84

Table B-2 Continued

Map #	Sample	Easting	Northing	Nd ppm	Sm ppm	Sm147	Nd143	WRP	Tdm (G)
BC Block (1.7-2.0 Ga)						Nd144	Nd144		
113	MX21	553026	5483441	23.1	4.85	0.1266	0.512056	0.010	1.72
	MX21R			28.7	5.96	0.1258	0.512060	0.010	1.70
	MX21R2			24.4	5.08	0.1256	0.512043	0.015	1.73
114	MX19	554461	5476630	22.5	3.90	0.1048	0.511778	0.011	1.77
115	SV8	562814	5463707	10.1	1.99	0.1191	0.511949	0.013	1.76
116	MB1***	558900	5451200	9.09	1.78	0.1240	0.511957	0.012	1.84
117	BC13*	563060	5458500	20.25	3.92	0.1170	0.511827	0.023	1.92
118	SV39	571680	5496260	31.0	6.52	0.1273	0.511977	0.016	1.88
119	SV35	576210	5481030	21.6	4.24	0.1184	0.511926	0.020	1.78
	SV35R			19.2	3.73	0.1172	0.511921	0.015	1.77
120	SV31	567330	5471370	27.7	5.12	0.1117	0.511784	0.012	1.88
121	BC14*	567560	5461070	15.23	2.83	0.1123	0.511891	0.011	1.73
122	SV7	570007	5460291	15.2	2.86	0.1133	0.511920	0.010	1.70
123	NS27**	571800	5459200	14.12	2.44	0.1045	0.511808	0.012	1.71
124	SV1	573078	5459472	20.0	3.93	0.1188	0.511945	0.013	1.76
125	SV2	584607	5461846	38.9	7.28	0.1130	0.511802	0.018	1.88
126	SV3	586772	5463491	35.6	6.67	0.1132	0.511774	0.018	1.92
127	SV4	591728	5461964	20.1	3.59	0.1079	0.511762	0.016	1.84
128	SV28	593390	5462770	39.5	8.22	0.1258	0.511931	0.011	1.93

Table B-3: Nd isotope analysis results for intermediate aged samples (1.65-1.69 Ga) in the study area.

Map #	Sample	Easting	Northing	Nd ppm	Sm ppm	Sm147	Nd143	WRP	Tdm (G)
Border (1.65-1.69 Ga)						Nd144	Nd144		
129	FV40	463281	5453423	47.9	9.01	0.1138	0.511960	0.011	1.65
130	FV33	467690	5448735	40.0	8.01	0.1210	0.512029	0.010	1.66
131	BC2*	522130	5491930	49.60	9.74	0.1187	0.511881	0.012	1.68
132	BC6*	547332	5461716	24.2	4.45	0.1110	0.511947	0.012	1.66
133	MX15	540790	5451217	9.6	1.76	0.1106	0.511924	0.013	1.65
134	MX13	542982	5449224	37.7	9.30	0.1491	0.512336	0.015	1.66
135	MX34	550356	5450697	36.0	7.37	0.1236	0.512047	0.013	1.68
136	SV13	562310	5455330	26.2	5.62	0.1298	0.512121	0.015	1.67

Table B-4: Major and trace element analyses

	Tdm (Ga)	SiO2	Al2O3	Fe2O3	MnO	MgO	CaO	Na2O	K2O	TiO2	P2O5	LOI	Total	Q	P	Sr	Y	Zr
Quebecia																		
BC 5	1.59	63.83	15.32	6.47	0.149	1.6	3.96	4.53	1.58	0.901	0.24	1.28	99.9	128	-183	397	21	145
BC 17	1.55	56.24	15.46	10.58	0.178	2.69	5.91	3.71	2.45	1.776	0.56	0.75	100.3	70	-173	370	48	379
NS 20	1.57	69.57	15.76	1.84	0.01	2.39	2.59	3.55	3.11	0.22	0.11	0.85	100.0	175	-95	570	13	104
NS 29	1.51	64.9	16.8	5.15	0.06	1.37	4.73	3.96	1.42	0.58	0.19	0.84	100.0	146	-182	829	13	271
NS 31	1.56	60.09	16.86	8.1	0.14	3.77	3.59	2.7	2.76	0.7	0.23	1.06	100.0	145	-92	387	26	186
NA 32a	1.56	68.94	15.9	4.02	0.05	1.78	2.61	3.03	2.42	0.6	0.18	0.47	100.0	203	-93	509	32	242
NS 32b	1.57	72.28	14.97	2.25	0.01	0.83	1.18	2.86	4.76	0.23	0.06	0.57	100.0	194	-12	204	26	180
MA 12	1.57	70.28	16.55	2.04	0.02	0.98	3.57	4.29	1.35	0.22	0.1	0.6	100.0	181	-173	542	6	84
MA 40	1.56	62.91	17.23	5.94	0.12	2.19	3.73	4.19	2.2	0.74	0.25	0.5	100.0	123	-155	521	23	197
MA 103	1.57	68.1	14.74	5.07	0.13	0.77	2.92	3.38	3.6	0.77	0.22	0.3	100.0	158	-85	261	52	381
MA 114	1.39	71.05	16.1	1.62	0.03	0.33	2.11	4.23	3.81	0.31	0.11	0.3	100.0	152	-93	481	5	156
MA 121	1.55	67.01	17.45	4.12	0.17	0.71	4.23	3.98	1.56	0.3	0.17	0.3	100.0	160	-171	609	15	83
MA 132	1.56	71.35	14.27	3.9	0.07	0.43	1.88	3.32	3.99	0.56	0.13	0.1	100.0	182	-56	187	50	280
LSJ 4	1.55	71.71	16.11	3.03	0.05	0.88	2.82	5.03	2.58	0.41	0.11		102.7	148	-158			
NS 9	1.55	67.74	17	3.33	0.01	0.94	3.77	4.47	1.67	0.36	0.16	0.55	100.0	152	-176	628	10	103
NS 11	1.54	71.22	15.9	1.93	0.13	0.84	2.48	4.46	2.07	0.2	0.1	0.67	100.0	178	-144	514	8	84
NS 18	1.58	64.43	16.78	5.54	0.1	1.2	2.27	3.3	4.58	0.73	0.34	0.73	100.0	127	-50	398	24	513
MA 153	1.56	71.46	16.15	2.48	0.01	0.24	2.93	3.64	2.41	0.28	0.1	0.3	100.0	193	-118	509	15	125
MA 178	1.56	69.26	15.59	3.66	0	1.09	3.41	3.82	2.33	0.39	0.15	0.3	100.0	171	-135	460	18	126
MA 182	1.57	71.98	15.44	2.35	0.06	0.55	1.46	3.17	4.46	0.33	0.1	0.1	100.0	185	-33	306	27	203
MA 199	1.56	67.73	17.64	3	0.01	0.89	3.97	4.59	1.44	0.37	0.16	0.2	100.0	150	-188	967	11	102
LSJ 1	1.54	65.53	16.76	5.76	0.1	1.78	3.42	3.92	1.6	0.46	0.27	0.4	100.0	163	-153	301	60	112
LSJ 2	1.59	67.95					2.38	2.38	5.29					160	-7	235	64	397
MB 2	1.54	66.06	13.29	5.72	0.11	2.29	3.96	3.19	3.24	1.06	0.18	0.9	100.0	148	-105	177	39	259
BC Block																		
BC 31	1.72	57.31	17.7	8.62	0.114	2.39	5.13	4.2	1.6	0.926	0.28	0.24	98.5	88	-193	448	27	193
BC 4	1.75	62.3	15.82	7.92	0.172	2.43	4.56	3.47	2.86	0.777	0.29	0.4	101.0	119	-133	385	26	132
BC 34	1.77	67.91	13.8	4.98	0.075	1.11	2.8	2.79	4.06	0.749	0.2	0.18	98.7	168	-54	187	26	237
BC 14	1.78	69.74	15.16	2.12	0.043	0.68	2.46	4.09	3.8	0.282	0.09	0.67	99.1	145	-95	811	14	110
BC 35	1.78	69.22	13.51	4.96	0.06	0.66	2.42	2.72	4.97	0.879	0.22	0.34	100.0	162	-25	450	64	940
BC 36	1.79	68.64	14.05	4.58	0.061	0.71	2.43	2.99	4.43	0.558	0.15	0.28	98.9	162	-46	176	43	267
BC 37	1.82	65.75	14.21	5.75	0.08	0.89	2.97	3.1	4.16	0.736	0.2	0.13	98.0	141	-65	207	43	319

Table B-4 Continued

	Tdm (Ga)	SiO2	Al2O3	Fe2O3	MnO	MgO	CaO	Na2O	K2O	TiO2	P2O5	LOI	Total	Q	P	Sr	Y	Zr
BC 15	1.83	71.45	15.25	1.22	0.042	0.34	2.26	4.71	2.35	0.124	0.03	0.48	98.3	168	-142	710	20	102
BC 41	1.84	69.6	13.81	4.47	0.056	0.63	2.12	2.75	5.26	0.531	0.13	0.21	99.6	161	-15	135	49	341
MB 1	1.84	73.98	15.24	1.23	0.06	0.02	1.57	4.37	3.06	0.1	0.07	0.3	100.0	186	-104	454	15	65
BC 32	1.86	68.12	13.56	4.79	0.054	0.69	2.61	2.94	4.5	0.656	0.16	0.52	98.6	157	-46	185	51	395
BC 38	1.88	69.2	14.35	4.21	0.055	0.66	2.22	2.86	5.5	0.57	0.14	0.4	100.2	149	-15	140	48	296
BC 45	1.88	68.67	14.12	4.97	0.067	0.81	2.59	2.93	4.88	0.668	0.16	0.24	100.1	152	-37	160	47	362
BC 13	1.92	70.46	15.09	3.08	0.056	1.05	2.23	3.43	3.61	0.363	0.1	0.76	100.2	177	-74	281	23	131
BC 43	1.93	70.01	14	4.23	0.053	0.66	2.17	2.73	5.33	0.582	0.12	0.37	100.3	162	-13	129	52	350
BC 1	1.96	70.32	13.92	4.33	0.055	0.66	2.37	2.56	5.71	0.596	0.14	0.34	101.0	158	-3	135	53	339
MA 25	1.86	65.06	15.98	5.47	0.06	1.62	2.91	2.84	3.45	0.69	0.22	1.7	100.0	162	-70	379	24	190
MA 42	1.87	72.42	15.39	2.04	0.01	0.18	2.37	3.79	3.29	0.21	0.1	0.2	100.0	182	-95	345	21	94
MA 58	1.97	69.93	14.17	4.34	0.1	0.59	2.27	2.83	4.86	0.56	0.15	0.2	100.0	167	-28	130	54	296
MA 67	1.87	70	14.03	4.28	0.06	0.55	2.41	2.76	4.87	0.6	0.14	0.3	100.0	168	-28	186	40	316
Berthe																		
MC 28	1.71	75.6	13.18	1.41	0.032	0.2	1.42	2.62	5.23	0.129	0.03	0.31	100.2	207	1	177	48	134
MC 12	1.72	73.42	12.9	3.94	0.077	0.54	1.92	2.36	4.74	0.405	0.15	0.23	100.7	208	-10	197	79	310
MC 23	1.76	76.73	12.15	2.05	0.028	0.29	1.55	2.01	5.18	0.373	0.09	0.27	100.7	233	18	158	25	297
MC 26	1.76	71.64	14.35	2.63	0.037	0.73	2.04	3.18	4.54	0.363	0.15	0.47	100.1	175	-42	328	15	208
MA 236.6	1.78	69.32	15.61	3.79	0.08	0.99	3.30	3.81	2.57	0.36	0.16		100.0	168	-127			
FT 23	1.8	65.07	16.13	5.71	0.12	1.37	3.38	4.70	2.85	0.53	0.15		100.0	109	-151			
FT 24	1.8	67.34	15.64	6.04	0.08	0.99	2.98	2.32	3.66	0.71	0.22		100.0	186	-50			
MC 11	1.83	75.34	13.16	1.07	0.024	0.13	0.98	2.43	6.08	0.079	0.02	0.21	99.5	199	33	129	11	19
FT 27	1.84	71.30	15.03	3.13	0.05	0.82	3.15	4.38	1.73	0.34	0.07		100.0	180	-161			
MA 240.7	1.86	74.16	14.38	2.33	0.03	0.32	1.88	3.49	2.96	0.39	0.05		100.0	214	-83			
MQ 25	1.87	68.21	14.66	5.52	0.08	0.59	2.97	2.93	4.06	0.73	0.24		100.0	163	-61			
MA 232.8	1.88	65.50	15.99	5.35	0.26	1.82	4.10	4.14	1.78	0.80	0.26		100.0	143	-169			
SK 8	1.9	72.54	14.58	2.8	0.059	0.79	3.89	3.88	1.17	0.265	0.1	0.21	100.3	207	-170	1061	13	210
MC 14	1.92	72.59	12.88	5.16	0.068	0.43	2.26	2.43	4.05	0.587	0.18	0.03	100.7	212	-33	167	36	415
SK 9	1.94	70.55	15.42	3.32	0.128	1.02	4.3	4.1	1.08	0.345	0.15	0.28	100.7	186	-186	698	14	213
MA 228.8	1.96	50.47	18.32	7.78	0.13	8.48	11.37	2.15	0.79	0.37	0.13		100.0	59	-255			
MC 6	1.96	67.63	15.25	4.95	0.065	1.46	2.93	2.96	3.37	0.75	0.27	0.3	99.9	174	-76	247	33	310
FT26	1.97	67.78	16.95	2.40	0.06	0.63	2.45	4.50	4.66	0.46	0.11		100.0	103	-90			
MC 24	2.09	70.87	13.36	5.07	0.071	0.51	2.17	2.18	5.04	0.567	0.2	0.09	100.1	190	-2	168	66	371

Table B-5: La Jolla Standard Analyses ($^{143}Nd/^{144}Nd$)

Date	$\frac{^{143}Nd}{^{144}Nd}$	Date	$\frac{^{143}Nd}{^{144}Nd}$
13/03/2012	.511856	16/09/2013	.511888
21/05/2012	.511874		.511854
	.511854		.511864
	.511868		.511853
21/05/2012	.511839	23/09/2013	.511853
11/06/2012	.511834		.511857
	.511861		.511850
18/06/2012	.511847	14/10/2013	.511869
02/07/2012	.511846	18/11/2013	.511846
23/07/2012	.511860		.511839
13/08/2012	.511844	02/12/2013	.511860
01/10/2012	.511854	23/12/2013	.511846
	.511876	27/01/2014	.511838
	.511836		.511829
	.511874	10/02/2014	.511857
21/10/2012	.511842		.511827
22/10/2012	.511823	12/05/2014	.511861
29/10/2012	.511848		.511859
12/11/2012	.511841		.511846
	.511865	20/05/2014	.511860
19/11/2012	.511851	2/06/2014	.511841
28/12/2012	.511870	8/07/2014	.511853
07/01/2013	.511873	11/08/2014	.511838
14/01/2013	.511876	08/12/2014	.511856
01/04/2013	.511856		.511851
06/05/2013	.511848	15/12/2014	.511856
	.511829		
	.511871		
03/06/2013	.511856		
10/06/2013	.511854		
	.511896		
1/07/2013	.511880		
	.511869		
22/07/2013	.511853		
	.511864		
12/08/2013	.511857		
26/08/2013	.511858		